# A Multifractal Model of Asset Returns*

Laurent Calvet
*Department of Economics, Harvard University*

Adlai Fisher
*Stern School of Business, New York University*

This Draft: November 10, 1999
First Draft: October 1996

*Littauer Center, Cambridge, MA 02138-3001, lcalvet@kuznets.harvard.edu; 44 West Fourth Street, New York, NY 10012-1126, afisher@stern.nyu.edu. We are very grateful to Benoit Mandelbrot for inspirational mentoring and exceptional advice during our years at Yale and beyond. His kindness and support have been invaluable to the development of this project. We acknowledge helpful comments from T. Andersen, D. Andrews, D. Backus, J. Campbell, P. Clark, T. Conley, R. Deo, F. Diebold, J. Geanakoplos, W. Goetzmann, O. Hart, P. de Lima, O. Linton, A. Lo, E. Maskin, R. Merton, P. C. B. Phillips, M. Richardson, S. Ross, R. Shiller, A. Shleifer, C. Sims, M. Taqqu, B. Zame, S. Zin, and seminar participants at numerous institutions, including Yale, NYU, Boston University, the Federal Reserve Board, Johns Hopkins, the Berkeley Program in Finance, the Harvard-MIT Theory Seminar, and the 1998 Summer Meeting of the Econometric Society. All remaining errors are our own.

**Abstract**

This paper investigates the *Multifractal Model of Asset Returns*, a continuous-time process that incorporates the thick tails and volatility persistence exhibited by many financial time series. The model is constructed by compounding a Brownian Motion with a multifractal time-deformation process. Return moments scale as a power law of the time horizon, a property confirmed for Deutschemark / U.S. Dollar exchange rates and several equity series. The model implies semi-martingale prices and thus precludes arbitrage in a standard two-asset economy. Volatility has long-memory, and the highest finite moment of returns can have any value greater than two. The local variability of the process is characterized by a renormalized probability density of local Hölder exponents. Unlike standard models, multifractal paths contain a multiplicity of these exponents within any time interval. We develop an estimation method, and infer a parsimonious generating mechanism for the exchange rate series. Simulated samples replicate the moment-scaling found in the data.

Keywords: Multifractal Model of Asset Returns, Compound Stochastic Process, Time Deformation, Scaling, Self-Similarity, Multifractal Spectrum, Stochastic Volatility

## 1. Introduction

This paper investigates the Multifractal Model of Asset Returns (MMAR), a continuous-time model that captures the thick tails and long-memory volatility persistence exhibited by many financial time series.[1] The model, which was first introduced in Mandelbrot (1997), is constructed by compounding a standard Brownian motion with a random time-deformation process.[2] Time-deformation is specified to be multifractal, which requires its moments to satisfy a generalized scaling rule, and produces clustering in volatility. The moments of returns scale as a power law in the time horizon, a property confirmed for Deutschemark / U.S. Dollar exchange rates, a U.S. equity index, and several individual stocks.

The model implies semi-martingale prices and uncorrelated returns, and thus precludes arbitrage in a standard two-asset economy. Volatility has long-memory, and the highest finite moment of returns can take any value greater than two. The unconditional distribution of returns changes with the time scale, and sample histograms may appear more thin-tailed at longer horizons. However, the unconditional distribution does not generally converge to a Gaussian with increasing horizon, and never converges to a Gaussian with decreasing horizon.

We show how to construct a class of candidate time-deformation processes as the limit of a simple iterative procedure called a multiplicative cascade. The cascade begins with a uniform distribution of volatility at a suitably long time horizon, and randomly concentrates volatility into progressively smaller time intervals. The construction follows the same rule at each stage of the cascade, which provides parsimony and ensures that returns satisfy moment-scaling. Volatility clustering is thus present at all frequencies, corresponding to the intuition that economic factors such as technology shocks, business cycles, earnings cycles, and liquidity shocks all have different time scales. We anticipate that fully rational equilibrium models can generate multifractal prices, either through exogenous

[1] Long memory is conveniently defined by hyperbolically declining autocorrelations. It was first analyzed in the context of fractional integration by Mandelbrot (1965, 1969, 1971, 1972*a*), Mandelbrot and van Ness (1968) and Mandelbrot and Wallis (1969). Long memory has been documented in squared and absolute returns for many financial data sets (Taylor, 1986; Ding, Granger, and Engle, 1993; Dacorogna *et al.*, 1993). Baillie (1996) provides a survey of long-memory in economics.

[2] An extension of the model, considered in Mandelbrot (1997) and in earlier working papers ([63], [21], [37]), compounds a *fractional* Brownian motion with a multifractal trading time. To simplify the discussion, we concentrate on the ordinary Brownian specification in Sections 1-4, and consider the more general model in Sections 5 and 6.

shocks with scaling patterns, or endogenously due to market incompleteness or informational cascades.

The MMAR introduces a fundamentally new class of processes to both finance and mathematics. Multifractal processes diffuse with continuous sample paths, but lie outside the class of Itô processes and fractional Brownian Motions. Whereas standard processes can be characterized by a single local scale that describes the magnitude of variations for successively smaller time increments, the MMAR contains a continuum of local scales in any time interval. The relative occurrences of each local scale are conveniently summarized in a renormalized probability density called the multifractal spectrum. Given a specification of the model, we provide a general rule for calculating the spectrum, and demonstrate its use in a number of examples. The applied researcher can estimate the spectrum through a transformation of the moments of data, and thus infer a specification of the model.

Our empirical work first examines the Deutschemark / U.S. Dollar ("DM/USD") exchange rate. We use a high frequency data set of approximately 1.5 million quotes collected over one year, and a twenty-three year sample of daily exchange rates. Moments of the data scale as predicted by the model for a remarkable range of time horizons. We estimate the multifractal spectrum and infer a generating mechanism that replicates DM/USD scaling in simulations. Further simulations show that GARCH and FIGARCH samples are less likely to reproduce these results. We find additional evidence of scaling in a U.S. equity index and five individual stocks.

Volatility modelling has received considerable attention in finance, and the most common approaches currently include numerous variants of the ARCH / GARCH class (Engle, 1982; Bollerslev, 1986) and the stochastic volatility approach (Wiggins, 1987). While weak memory is typical of earlier models, long-memory in squared returns is present in FIGARCH (Baillie, Bollerslev and Mikkelsen, 1996) and the Long Memory Stochastic Volatility (LMSV) process proposed by Breidt, Crato, and DeLima (1997). The multifractal model is analogous to previous stochastic volatility models in many respects, but extends the characterization of randomness in volatility.[3]

By design, the MMAR incorporates sufficient intermittent bursts of extreme volatility to fully capture a wide variety of tail behaviors, while maintaining a

[3]While standard stochastic volatility formulations consider infinitesimals of the form $\sigma(t)(dt)^{1/2}$, the MMAR permits non-standard infinitesimals $c(t)\,(dt)^{\alpha(t)}$. This is further discussed in Section 4.

diffusion process. In contrast, previous research has found it necessary to modify the conditional distribution of returns to fit thick-tailed data. These adaptations include the Student-$t$ specification (Bollerslev, 1987) and non-parametric specifications (Engle and Gonzalez-Rivera, 1991). In continuous time, the problem of modeling thick tails is more acute, and is typically addressed by incorporating an independent stochastic jump process.[4]

The multifractal model differs most fundamentally from previous volatility models in its scaling properties. The emphasis on scaling can be traced back to the work of Mandelbrot (1963) and Fama (1963) for extreme variations, and Mandelbrot and van Ness (1967) for long-memory. Multifractality, a form of generalized scaling that includes both extreme variations and long-memory, was first developed in models of turbulent dissipation (Mandelbrot, 1972*b*, 1974). The MMAR brings generalized scaling to finance by extending multifractality from measures to processes.

Section 1.1 discusses the relation between the MMAR and earlier scaling models. Section 2 defines multifractals, and demonstrates their construction through a number of simple examples. Section 3 formalizes the MMAR by compounding a Brownian motion with a continuous time-deformation process. Section 4 develops the concept of local scale and shows that multifractal processes can take a continuum of such values. We also present the multifractal spectrum, which provides a convenient renormalized probability density for the distribution of local scales. Section 5 extends the model to permit long-memory in the levels of returns. This allows testing of the martingale hypothesis and may be useful in modelling economic series other than exchange-rates and equities. In Section 6, we verify the multifractal scaling rule for DM/USD exchange rates, and estimate the spectrum of local scales. We infer a data-generating process and show that simulated samples replicate the scaling features of the data. Evidence of multifractal scaling is also found in a U.S. equity index and five individual stocks. In Section 7, we summarize our results and discuss possible extensions.

This paper simplifies the discussion and extends the results of three earlier working papers ([63], [21], [37]). Throughout the text, we refer to them respectively as MFC, CFM, and FCM, signifying the various permutations of the authors.

[4]Bates (1995, 1996) finds that standard diffusions cannot produce tails sufficient to explain the implied volatility smile in option prices, and recommends the incorporation of jumps. One potentially undesirable consequence of this approach is that the most extreme fluctuations are then disconnected from volatility.

### 1.1. Roots of the MMAR

The multifractal model combines several elements of previous research on financial time series. First, the MMAR generates fat tails in the unconditional distribution of returns, as in the $L$-stable processes of Mandelbrot (1963) and Fama (1963).[5] The MMAR improves on this earlier model by allowing a finite variance,[6] and modeling one of the main features of financial markets - fluctuations in volatility.

Second, the multifractal model has long memory in the absolute value of returns, but the returns themselves can have a white spectrum. Long memory is the characteristic feature of *fractional Brownian motion* (FBM), introduced by Mandelbrot and van Ness (1968). A FBM, denoted $B_H(t)$, has continuous sample paths, as well as Gaussian and possibly dependent increments. The FBM is an ordinary Brownian motion for $H = 1/2$, is antipersistent when $0 < H < 1/2$, and displays persistence and long memory when $1/2 < H < 1$. Granger and Joyeux (1980) and Hosking (1981) introduced ARFIMA, a discrete time generalization of the FBM which advanced the use of long memory in economics. FBM and ARFIMA do not permit the independent modeling of persistence in returns and long memory in volatility.[7] More recent models, such as FIGARCH and LMSV, contain long memory in volatility and uncorrelated returns in discrete time. The MMAR has the same properties, but in a parsimonious, continuous-time setting.

The third essential component of the multifractal market model is the concept of *trading time*, introduced by Mandelbrot and Taylor (1967).

**Definition 1.** *Let $\{B(t)\}$ be a stochastic process, and $\theta(t)$ an increasing function of $t$. The process*

$$X(t) \equiv B[\theta(t)]$$

*is called a* compound *or* subordinated *process. The index $t$ denotes* clock time, *and $\theta(t)$ is called* trading time *or the* time deformation process.

When the directing process $B$ is a martingale, fluctuations in trading time cause speeding up or slowing down of the process $X(t)$ without influencing its direction.

[5] Recent applications of the $L$-stable model to foreign exchange and stock prices include Koedijk and Kool (1992), Belkacem, Lévy-Véhel and Walter (1995), and Phillips, McFarland and McMahon (1996).

[6] In the leading case considered in this paper, the critical exponent $q_{crit}$ can take any value in $(2, \infty]$.

[7] Taqqu (1975) establishes that $B_H(t)$ has long memory in the absolute value of increments when $H > 1/2$.

Compounding[8] can thus separate the direction and the size of price movements, and has been used in the literature to model the unobserved natural time-scale of economic series (Mandelbrot and Taylor, 1967; Clark, 1973; Mandelbrot, 1973; Stock, 1987, 1988). More recently, this method has been used to build models integrating seasonal factors (Dacorogna *et al.*, 1993; Müller *et al.*, 1995), and measures of market activity (Ghysels, Gouriéroux, and Jasiak, 1996). The MMAR also incorporates compounding and the primary innovation is the specification of trading time $\theta$ as multifractal. While this is not a structural model of trade, future work may specify the trading time $\theta$ as a function of observable data.

Finally, the MMAR generalizes the concept of scale-consistency, in the sense that a well-defined scaling rule relates returns over different sampling intervals. Mandelbrot (1963), followed by Fama (1963), suggested that the shape of the distribution of returns should be the same when the time scale is changed, or more formally:

**Definition 2.** *A random process* $\{X(t)\}$ *that satisfies*

$$\{X(ct_1), ..., X(ct_k)\} \stackrel{d}{=} \{c^H X(t_1), ..., c^H X(t_k)\}$$

*for some* $H > 0$ *and all* $c, k, t_1, ..., t_k \geq 0$, *is called* self-affine.[9] *The number* $H$ *is the* self-affinity index, *or* scaling exponent, *of the process* $\{X(t)\}$.

The Brownian motion, the $L$-stable process and the FBM are the main examples of self-affine processes in finance. Empirical evidence suggests that many financial series are not exactly self-affine, but instead have thinner tails and become less peaked in the bells when the sampling interval increases. The MMAR captures this feature, as well as a generalized version of self-affinity exhibited by the data. The multifractal process does not necessarily converge to a Gaussian at long sampling intervals, and is sufficiently flexible to model a wide range of financial time series.

[8] In mathematics, subordination differs from compounding, and requires that $\theta(t)$ have independent increments (Bochner, 1955; Feller, 1968). The concept of subordination has evolved differently in financial economics, and now encompasses any generic time deformation process.

[9] Self-affine processes are sometimes called self-similar in the literature.

## 2. Multifractal Measures and Processes

The MMAR is constructed in Section 3 by compounding a Brownian motion $B(t)$ with a stochastic trading time $\theta(t)$:

$$\ln P(t) - \ln P(0) = B[\theta(t)],$$

where $\theta(t)$ is a random increasing function or, equivalently, the cumulative distribution function (c.d.f.) of a random measure $\mu$. In order to capture the outliers and volatility persistence of many financial time series, we specify the measure $\mu$ to be multifractal, a concept which we now present.

### 2.1. The Binomial Measure

In the spirit of fractal geometry, multifractal measures are built by iterating an elementary procedure, called a *multiplicative cascade*. The simplest multifractal is the binomial measure[10] on the compact interval $[0, 1]$. Consider the uniform probability measure $\mu_0$ on $[0, 1]$, and two positive numbers $m_0$ and $m_1$ adding up to 1. In the first step of the cascade, we define a new measure $\mu_1$ by uniformly spreading the mass $m_0$ on the *left* subinterval $[0, 1/2]$, and the mass $m_1$ on the *right* subinterval $[1/2, 1]$. The density of $\mu_1$ is now a step function, as illustrated in Figure 1*a*.

In the second stage of the cascade, we split the interval $[0, 1/2]$ into two subintervals of equal length, $[0, 1/4]$ and $[1/4, 1/2]$. The left subinterval $[0, 1/4]$ receives a fraction $m_0$ of the mass $\mu_1[0, 1/2]$, while the right subinterval receives a fraction $m_1$. Applying this again to the interval $[1/2, 1]$, we obtain a new measure $\mu_2$, which satisfies

$$\begin{aligned} \mu_2[0, 1/4] &= m_0 m_0, \qquad & \mu_2[1/4, 1/2] &= m_0 m_1, \\ \mu_2[1/2, 3/4] &= m_1 m_0, & \mu_2[3/4, 1] &= m_1 m_1. \end{aligned}$$

Iteration of this procedure generates an infinite sequence of measures $(\mu_k)$, which converges[11] to the binomial measure $\mu$. Figure 1*b* illustrates the density of the measure $\mu_4$ obtained after $k = 4$ steps of the recursion.

We now introduce notation that aids our treatment of the binomial measure $\mu$. For any $\eta_1, .., \eta_k \in \{0, 1\}$, we denote by $I_{\eta_1,..,\eta_k}$ the interval of length $2^{-k}$ with lower endpoint

$$t_{\eta_1,..,\eta_k} = \eta_1 2^{-1} + ... + \eta_k 2^{-k}. \tag{2.1}$$

[10] The binomial measure is sometimes called the Bernoulli or Besicovitch measure.

[11] In the sense of weak convergence.

With this definition, each vector $(\eta_1, .., \eta_k)$ indexes an interval used in the $k$th stage of the construction. For example, the first step of the cascade uses the two intervals $I_0 = [0, 1/2]$ and $I_1 = [1/2, 1]$, while the second stage considers the subintervals $I_{0,0} = [0, 1/4]$, $I_{0,1} = [1/4, 1/2]$, $I_{1,0} = [1/2, 3/4]$, and $I_{1,1} = [3/4, 1]$. We note that subinterval $I_{\eta_1,\eta_2}$ is located inside the larger interval $I_{\eta_1}$ at a position determined by $\eta_2$. More generally, a "stage $k$" interval $I_{\eta_1,..,\eta_k}$ is contained in the "stage $k-1$" interval $I_{\eta_1,..,\eta_{k-1}}$, and by recursion, $I_{\eta_1,..,\eta_k} \subset I_{\eta_1,..,\eta_{k-1}} \subset ... \subset I_{\eta_1}$. These notations make it transparent that the construction involves a countable set of grid points and intervals. A number $t \in [0, 1]$ is called *dyadic* if $t = 1$ or $t = t_{\eta_1,..,\eta_k}$ for some finite $k$. Similarly, a *dyadic* interval $I \subseteq [0, 1]$ has dyadic endpoints. The intervals $I_{\eta_1,..,\eta_k}$ and grid points $t_{\eta_1,..,\eta_k}$ in the construction are all dyadic.

We now use this notation to analyze the properties of $\mu$. Consider the dyadic interval $[t, t + 2^{-k}]$, where

$$t = t_{\eta_1,..,\eta_k} = \eta_1 2^{-1} + ... + \eta_k 2^{-k}$$

and $\eta_1, ..., \eta_k \in \{0, 1\}$. Let $\varphi_0$ and $\varphi_1$ denote the relative frequencies of 0s and 1s in $(\eta_1, ..., \eta_k)$. The measure of the dyadic interval simplifies to

$$\mu[t, t + 2^{-k}] = m_0^{k\varphi_0} m_1^{k\varphi_1}.$$

Like many multifractals, the binomial is a continuous but singular probability measure; it thus has no density and no point mass. We also observe that since $m_0 + m_1 = 1$, each stage of the construction preserves the mass of split dyadic intervals.

This construction can be extended in several ways. For instance at each stage of the cascade, intervals can be split into $b > 2$ intervals of equal size. Subintervals, indexed from left to right by $\beta$ $(0 \leq \beta \leq b-1)$, receive fractions of the total mass equal to $m_0, .., m_{b-1}$. By the conservation of mass, these fractions, also called *multipliers*, add up to one: $\sum m_\beta = 1$. This defines the class of *multinomial* measures, which are discussed in Mandelbrot (1989a) and Evertsz and Mandelbrot (1992).

Another extension randomizes the allocation of mass between subintervals at each step of the iteration. The multiplier of each subinterval is a discrete random variable $M_\beta$ that takes values $m_0, m_1, ..., m_{b-1}$ with probabilities $p_0, .., p_{b-1}$. The preservation of mass imposes the additivity constraint: $\sum M_\beta = 1$. Figure 1*c* shows the random density obtained after $k = 10$ iterations with parameters

$b = 2$, $p = p_0 = 0.5$ and $m_0 = 0.6$. This density, which represents the flow of trading time, begins to show the properties we desire in modeling financial volatility. The occasional bursts of trading time generate thick tails in the compound price process, and their clustering generates volatility persistence. Because the reshuffling of mass follows the same rule at each stage of the cascade, volatility clustering is present at all time scales.

### 2.2. Multiplicative Measures

Another extension of the multinomial allows non-negative multipliers $M_\beta$ ($0 \leq \beta \leq b-1$) that can have arbitrary probability distributions. For simplicity, we assume identically distributed multipliers drawn from a random variable $M$. The limit *multiplicative measure* is called *conservative* when mass is conserved at each stage of the construction: $\sum M_\beta = 1$, or *canonical* when it is only preserved "on average": $\mathbb{E}(\sum M_\beta) = 1$ or $\mathbb{E}M = 1/b$.

Consider the generating cascade of a *conservative* measure $\mu$. In the first stage, we partition the unit interval $[0, 1]$ into $b$-adic cells of length $1/b$, and allocate random masses $M_0, .., M_{b-1}$ to each of these cells. By a repetition of this scheme, the $b$-adic cell with length $\Delta t = b^{-k}$ and lower endpoint $t_{\eta_1,..,\eta_k} = \sum_{i=1}^{k} \eta_i b^{-i}$, $\eta_i \in \{0, .., b-1\}$ for all $i$, has measure

$$\mu(\Delta t) = M(\eta_1)M(\eta_1, \eta_2)...M(\eta_1, ..., \eta_k), \tag{2.2}$$

Multipliers defined at different stages of the cascade are chosen to be statistically independent, and relation (2.2) implies that $\mathbb{E}[\mu(\Delta t)^q] = [\mathbb{E}(M^q)]^k$, or equivalently

$$\mathbb{E}[\mu(\Delta t)^q] = (\Delta t)^{\tau(q)+1}, \tag{2.3}$$

where $\tau(q) = -\log_b \mathbb{E}(M^q) - 1$. The moment of an interval's measure is thus a power functions of the length $\Delta t$. This important scaling rule characterizes multifractals.

Modifying the previous construction, we generate a *canonical* measure $\mu$ by imposing that the multipliers $M_\beta$ be statistically independent *within* each stage of the cascade. When $\mathbb{E}M_\beta = \mathbb{E}M = 1/b$, each iteration of the cascade conserves mass *on average*, and the mass of the unit interval is a random variable $\Omega$.[12] The

[12] The random variable $\Omega$ has interesting distributional and tail properties that are discussed in Mandelbrot (1989a). $\Omega$ is non negative, has a critical moment $q_{crit}$, $1 < q_{crit} < \infty$, and a Paretian tail: $\mathbb{P}\{\Omega > \omega\} \sim C_1 \omega^{-q_{crit}}$ as $\omega \to +\infty$, where $C_1$ is a positive number. The

mass of a $b$-adic cell takes the form

$$\mu(\Delta t) = \Omega(\eta_1, ..., \eta_k) M(\eta_1) M(\eta_1, \eta_2) ... M(\eta_1, ..., \eta_k),$$

where $\Omega(\eta_1, ..., \eta_k)$ has the same distribution as $\Omega$. The measure $\mu$ thus satisfies the scaling relationship

$$\mathbb{E}[\mu(\Delta t)^q] = \mathbb{E}(\Omega^q) \, (\Delta t)^{\tau(q)+1}, \tag{2.4}$$

which generalizes (2.3). We note that multiplicative measures constructed so far are *grid-bound,* in the sense that the scaling rule (2.4) holds only when $t = t_{\eta_1,..,\eta_k}$ and $\Delta t = b^{-l}$, $l \geq k$. Let $\mathcal{D}$ denote the set of couples $(t, \Delta t)$ satisfying scaling rule (2.4). $\mathcal{D}$ has interesting topological properties that are summarized in Condition 1 of Appendix 8.1. Alternatively, we can consider *grid-free* random measures that satisfy scaling rule (2.4) for all admissible values of $(t, \Delta t)$ (Mandelbrot, 1989a). This leads to the following

**Definition 3.** *A random measure $\mu$ defined on $[0, 1]$ is called* multifractal *if it satisfies*

$$\mathbb{E}(\mu[t, t + \Delta t]^q) = c(q)(\Delta t)^{\tau(q)+1} \qquad \textit{for all } (t, \Delta t) \in \mathcal{D},\ q \in \mathcal{Q},$$

*where $\mathcal{D}$ is a subset of $[0, 1] \times [0, 1]$, $\mathcal{Q}$ is an interval, and $\tau(q)$ and $c(q)$ are functions with domain $\mathcal{Q}$. Moreover, $[0, 1] \subseteq \mathcal{Q}$, and $\mathcal{D}$ satisfies Condition 1.*[13]

Maintaining the distinction between grid-bound and grid-free measures would prove very cumbersome and lead to unnecessary technicalities. For this reason, the difference between the two classes is henceforth neglected. This helps focus on the key elements of the model: scaling, compounding and long memory.

### 2.3. Multifractal Processes

We now extend multifractality from measures to stochastic processes, a formalization new to the mathematics and finance literature. We find it convenient to define multifractal processes in terms of moments, because of its direct graphical and testable implications.

---

cascade construction also implies that $\Omega$ satisfies the invariance relation $\sum_{i=1}^{b} M_i \Omega_i \stackrel{d}{=} \Omega$, where $M_1, .., M_b$, $\Omega_1, .., \Omega_b$ are independent copies of the random variables $M$ and $\Omega$.

[13] Condition 1 is defined in the Appendix.

**Definition 4.** *A stochastic process* $\{X(t)\}$ *is called* multifractal *if it has stationary increments and satisfies*

$$\mathbb{E}\left(|X(t)|^q\right) = c(q)t^{\tau(q)+1}, \text{ for all } t \in \mathcal{T},\ q \in \mathcal{Q}, \tag{2.5}$$

*where* $\mathcal{T}$ *and* $\mathcal{Q}$ *are intervals on the real line,* $\tau(q)$ *and* $c(q)$ *are functions with domain* $\mathcal{Q}$*. Moreover,* $\mathcal{T}$ *and* $\mathcal{Q}$ *have positive lengths, and* $0 \in \mathcal{T}$, $[0,1] \subseteq \mathcal{Q}$.

The function $\tau(q)$ is called the *scaling function* of the multifractal process. Setting $q = 0$ in condition (2.5), we see that all scaling functions have the same intercept $\tau(0) = -1$. In addition, it is easy to show

**Proposition 1.** *The scaling function* $\tau(q)$ *is concave.*

**Proof:** See Appendix. ■

We will see that the distinction between linear and nonlinear scaling functions $\tau(q)$ is particularly important in this framework.

Self-affine process $\{X(t)\}$ are multifractal and have a linear scaling function $\tau(q)$, as is now shown. Denoting by $H$ the self-affinity index, we observe that the invariance condition $X(t) \overset{d}{=} t^H X(1)$ implies $\mathbb{E}\left(|X(t)|^q\right) = t^{Hq}\mathbb{E}\left(|X(1)|^q\right)$, and scaling rule (2.5) therefore holds with $c(q) = \mathbb{E}\left(|X(1)|^q\right)$ and

$$\tau(q) = Hq - 1.$$

In this special case, the scaling function $\tau(q)$ is linear and fully determined by its index $H$. More generally, linear scaling functions $\tau(q)$ are determined by a unique parameter, their slope, and the corresponding processes are called *uniscaling* or *unifractal*.

Uniscaling processes, which may seem appealing for their simplicity, do not satisfactorily model many financial time series. This is because most financial data sets have thinner tails and become less peaked in the bell when the sampling intervals $\Delta t$ increases. In this paper, we focus on *multiscaling* processes, which have a nonlinear $\tau(q)$. The proof of Proposition 1 shows that these processes are only defined on *bounded* time intervals $\mathcal{T}$, a limitation of little consequence in finance since $\mathcal{T}$ can have arbitrarily length. Multiscaling processes provide a parsimonious framework with strict moment conditions, and enough flexibility to model a wide range of financial prices.

## 3. The Multifractal Model of Asset Returns

We now formalize construction of the MMAR. Consider the price of a financial asset $P(t)$ on a bounded interval $[0, T]$, and define the *log-price* process

$$X(t) \equiv \ln P(t) - \ln P(0).$$

We model $X(t)$ by compounding a Brownian motion with a multifractal trading time:

**Assumption 1.** *$X(t)$ is a compound process*

$$X(t) \equiv B[\theta(t)]$$

*where $B(t)$ is a Brownian motion, and $\theta(t)$ is a stochastic trading time.*

**Assumption 2.** *Trading time $\theta(t)$ is the c.d.f. of a multifractal measure $\mu$ defined on $[0, T]$.*

**Assumption 3.** *The processes $\{B(t)\}$ and $\{\theta(t)\}$ are independent.*

This construction, which is new to both mathematics and finance, generates a large class of multifractal processes. We will show that the price process is a semi-martingale, which implies the absence of arbitrage in simple cases. A straightforward generalization of the MMAR weakens Assumption 1 to a FBM $B_H(t)$, and is developed in Section 5. In Assumption 2, the multifractal measure $\mu$ can be multinomial or multiplicative, which implies a continuous trading time $\theta(t)$ with non-decreasing paths and stationary increments. Assumption 3 ensures that the unconditional distribution of returns is symmetric. Weakening this assumption allows leverage effects, as in EGARCH (Nelson, 1991) and Glosten, Jagannathan and Runkle (1993), and is a promising area of future research.

Under the above assumptions,

**Theorem 1.** *The log-price $X(t)$ is a multifractal process with stationary increments and scaling function $\tau_X(q) \equiv \tau_\theta(q/2)$.*

**Proof:** See Appendix. ■

Trading time controls the tail properties of the process $X(t)$. As shown in the proof, the $q$-th moment of $X$ exists if (and only if) the process $\theta$ has a moment

of order $q/2$. In particular if $\mathbb{E}\,|X(t)|^q$ is finite for some instant $t$, then it is finite for all $t$, and we therefore drop the time index in the moments of multifractal processes.

The tails of $X(t)$ have different properties if the generating measure is conservative or canonical. If $\mu$ is *conservative*, trading time is bounded, and the process $X(t)$ has finite moments of all (non-negative) order. Conservative measures thus generate "mild" processes with relatively thin tails. Conversely, the total mass $\theta(T) \equiv \mu[0,T]$ of a *canonical* measure is a random variable with Paretian tails (Mandelbrot, 1972; Guivarc'h, 1987). In particular, there exists a *critical exponent* $q_{crit}(\theta) > 1$ for trading time such that $\mathbb{E}\theta^q$ is finite when $0 \leq q < q_{crit}(\theta)$, and infinite when $q \geq q_{crit}(\theta)$.[14] The log-price $X(t)$ then has infinite moments, and is accordingly called "wild". Note however that $X(t)$ always has finite variance, since $q_{crit}(X) = 2q_{crit}(\theta) > 2$. Overall, the MMAR has enough flexibility to accommodate a wide variety of tail behaviors.

The model also has an appealing autocorrelation structure.

**Theorem 2.** *The price $\{P(t)\}$ is a semi-martingale (with respect to its natural filtration), and the process $\{X(t)\}$ is a martingale with finite variance and thus uncorrelated increments.*

**Proof:** See Appendix. ■

The MMAR thus implies that asset returns have a white spectrum, a property which has been extensively discussed in the market efficiency literature.[15]

The price $P(t)$ is a semi-martingale,[16] which has important consequences for arbitrage.[17] Consider for instance the *two asset economy* consisting of the multifractal security with price $P(t)$, and a riskless bond with constant rate of return $r$. Following Harrison and Kreps (1979), we can analyze if arbitrage profits can

[14] We also know that the scaling function $\tau_\theta(q)$ is negative when $0 < q < 1$, and positive when $1 < q < q_{crit}(\theta)$.

[15] See Campbell, Lo and MacKinlay (1997) for a recent discussion of these concepts. We also note that immediate extensions of the MMAR could add trends or other predictable components to the compound process in order to fit financial time series other than exchange rates.

[16] Since the process $X(t) = \ln P(t)$ is a martingale, Jensen's inequality implies that the price $P(t)$ is a submartingale but *not* a martingale. This result is of course not specific to the MMAR, and holds for many Itô processes used in finance.

[17] See Dothan (1990) for a discussion of semi-martingales in the context of finance.

be made by frequently rebalancing a portfolio of these two securities. Theorem 2 directly implies

**Theorem 3.** *There are no arbitrage opportunities in the two asset economy.*

This suggests that future research may seek to embed the MMAR in standard financial models. Since the price $P(t)$ is a semi-martingale, stochastic integration can be used to calculate the gains from trading multifractal assets, which in future work will greatly help us develop portfolio selection and option pricing theory. Further research will also seek to integrate multifractality into equilibrium theory. We may thus obtain the MMAR in a general equilibrium model with *exogenous* multifractal technological shocks, in the spirit of Cox, Ingersoll and Ross (1985). Such a methodology is justified by the multifractality of many natural phenomena, such as weather patterns, and will help build new economic models of asset and commodity prices. Another line of research could also obtain multifractality as an *endogenous* equilibrium property, which might stem from the incompleteness of financial markets (Calvet, 1998) or informational cascades (Gennotte and Leland, 1990; Bikhchandani, Hirshleifer and Welch, 1992; Jacklin, Kleidon and Pfleiderer, 1992; Bulow and Klemperer, 1994; Avery and Zemsky, 1998).

Recent research focuses not only on predictability in returns, but also on persistence in the size of price changes. The MMAR adds to this literature by proposing a continuous time model with long memory in volatility. Because the price process is only defined on a *bounded* time range, the definition of long memory seems problematic. We note, however, that for any stochastic process $Z$ with stationary increments $Z(a, \Delta t) \equiv Z(a + \Delta t) - Z(t)$, the *autocovariance in levels*

$$\delta_Z(t, q) = Cov(|Z(a, \Delta t)|^q, |Z(a + t, \Delta t)|^q),$$

quantifies the dependence in the size of the process's increments. It is well-defined when $\mathbb{E}|Z(a, \Delta t)|^{2q}$ is finite. For a fixed $q$, we say that the process has *long memory in the size of increments* if the autocovariance in levels is hyperbolic in $t$ when $t/\Delta t \to \infty$. When the process $Z$ is multifractal, this concept does not depend on the particular choice of $q$.[18] It is easy to show that when $\mu$ is a multiplicative measure,

**Theorem 4.** *Trading time $\theta(t)$ and log-price $X(t)$ have long memory in the size of increments.*

[18]Provided that $\mathbb{E}|Z(a, \Delta t)|^{2q} < \infty$, as is implicitly assumed in the rest of the paper.

**Proof:** See Appendix. ■

This result can be illustrated graphically. Figure 2 shows simulated first differences when $\theta(t)$ the c.d.f. of a randomized binomial measure with multiplier $m_0 = 0.6$. The simulated returns displays marked temporal heterogeneity at all time scales and intermittent large fluctuations.

The MMAR is thus a flexible continuous time framework that accommodates long memory in volatility, a variety of tail behaviors, and either unpredictability or long memory in returns. Furthermore, the multifractal model contains volatility persistence at all time frequencies. Table 1 places the MMAR within the existing literature on financial time series.

Table 1: Typical Characteristics for Models of Financial Returns

| Volatility Clustering Consistent with Martingale Price | Volatility Clustering Implies Predictable Price | PROPERTIES |
|---|---|---|
| MMAR | FBM | long memory continuous time |
| FIGARCH | ARFIMA* | long memory discrete time |
| GARCH | ARMA* | short memory discrete time |

∗ Asymptotically, ARMA scales like Brownian Motion, and ARFIMA like FBM.

## 4. The Multifractal Spectrum

This section examines the geometric properties of sample paths in the MMAR. While we previously focused on *global* properties such as moments and autocovariances, we now adopt a more *local* viewpoint and examine the regularity of realized paths around a given instant. The analysis builds on a concept borrowed from real analysis, the local Hölder exponent. On a given path, the infinitesimal variation in price around a date $t$ is heuristically of the form[19]

$$|\ln P(t+dt) - \ln P(t)| \sim C_t(dt)^{\alpha(t)},$$

[19] The expression $(dt)^{\alpha(t)}$ is an example of "non-standard infinitesimal", as developed by Abraham Robinson.

where $\alpha(t)$ and $C_t$ are respectively called the *local Hölder exponent* and the *prefactor* at $t$. As is apparent in this definition, the exponent $\alpha(t)$ quantifies the scaling properties of the process at a given point in time, and is also called the *local scale* of the process at $t$.

In continuous Itô diffusions, the Hölder exponent takes the unique value $\alpha(t) = 1/2$ at every instant.[20] For this reason, traditional research obtains time variations in market volatility through changes in the prefactor $C_t$.[21] In contrast, the MMAR contains a *continuum* of local scales $\alpha(t)$ within any finite time interval. Thus, multifractal processes are *not* continuous Itô diffusions and cannot be generated by standard techniques. Fractal geometry imposes that in the MMAR, the instants $\{t : \alpha(t) < \alpha\}$ with local scale less than $\alpha$ cluster in clock time, thus accounting for the concentration of price changes in our model. The relative frequency of the local exponents can be represented by a renormalized density called the *multifractal spectrum*. For a broad class of multifractals, we calculate this spectrum by an application of Large Deviation Theory.

### 4.1. Local Scales

We first formalize the concept of local scale.

**Definition 5.** *Let $g$ be a function defined on the neighborhood of a given date $t$. The number*

$$\alpha(t) = Sup\ \{\beta \geq 0 : |g(t + \triangle t) - g(t)| = O(|\triangle t|^{\beta}) \text{ as } \triangle t \to 0\}$$

*is called the* local Hölder exponent *or* local scale *of $g$ at $t$.*

Lower values of the local scale thus correspond to more abrupt variations in the path. The exponent $\alpha(t)$ is non-negative when the function $g$ is bounded around $t$, as is always the case in this paper. Definition 5 readily extends to measures on the real line. At a given date $t$, a measure simply has the local exponent of its c.d.f.

We can easily compute Hölder exponents for many functions and processes. For instance the local scale of a function is 0 at points of discontinuity, and 1 at (non-singular) differentiable points. Smooth functions thus have integral

[20] More precisely, the set $\{t : \alpha(t) \neq 1/2\}$ of instants with a local scale different from $1/2$ has a Hausdorff-Besicovitch measure (and therefore a Lebesgue measure) equal to zero. This set can thus be neglected in our analysis. See Kahane (1997) for a recent survey of this topic.

[21] See Rossi (1997) for a recent presentation of these advances.

exponents almost everywhere. On the other hand, the unique scale $\alpha(t) = 1/2$ is observed on the jagged sample paths of a Brownian motion or of a continuous Itô diffusion. Similarly, a FBM $B_H(t)$ is characterized by a unique exponent $\alpha(t) = H$. Thus, the continuous processes typically used in finance each have a unique Hölder exponent. In contrast, multifractal processes contain a continuum of local scales. The mathematics literature has developed a convenient representation for the distribution of Hölder exponents within a multifractal measure. This representation, called the multifractal spectrum, is a function $f(\alpha)$ that we now describe.

From Definition 5, the Hölder exponent $\alpha(t)$ is the limsup of the ratio

$$\ln |g(t, \triangle t)| / \ln(\triangle t) \text{ as } \triangle t \to 0,$$

where, consistent with previous notation, $g(t, \triangle t) \equiv g(t + \triangle t) - g(t)$. This suggests estimating the distribution of the local scale $\alpha(t)$ at a random instant. For increasing $k \geq 1$, we partition $[0, T]$ into $b^k$ subintervals $[t_i, t_i + \Delta t]$, where length $\triangle t = b^{-k}T$, and calculate for each subinterval the *coarse Hölder exponent*

$$\alpha_k(t_i) \equiv \ln |g(t_i, \triangle t)| / \ln \triangle t.$$

This operation generates a set $\{\alpha_k(t_i)\}$ of $b^k$ observations. We then divide the range of $\alpha$s into small intervals of length $\triangle\alpha$, and denote by $N_k(\alpha)$ the number of coarse exponents contained in $(\alpha, \alpha + \triangle\alpha]$. It would then be natural to calculate a histogram with the relative frequencies $N_k(\alpha)/b^k$, which converge as $k \to \infty$ to the probability that a random instant $t$ has Hölder exponent $\alpha$. Using this method, however, the histogram would degenerate into a spike and thus fail to distinguish the MMAR from traditional processes. This is because multifractals typically have a dominant exponent $\alpha_0$, in the sense that $\alpha(t) = \alpha_0$ at almost every instant. Mandelbrot (1989a) instead suggested

**Definition 6.** *The limit*

$$f(\alpha) \equiv \lim \left\{ \frac{\ln N_k(\alpha)}{\ln b^k} \right\} \text{ as } k \to \infty \tag{4.1}$$

*represents a renormalized probability distribution of local Hölder exponents, and is called the* multifractal spectrum.

For instance if $b = 3$ and $N_k(\alpha) = 2^k$, the frequency $N_k(\alpha)/b^k = (2/3)^k$ vanishes to zero as $k \to \infty$, while the ratio $\ln N_k(\alpha)/\ln b^k = \ln 2/\ln 3$ is a positive constant.

Histograms can then be plotted by applying the two methods for many values of $\alpha$. With a multifractal, the first technique degenerates into a spike, while the second converges to a function $f(\alpha)$ of the Hölder exponent. The multifractal spectrum thus helps to identify events that happen many times in the construction but at a vanishing frequency. We also note that Definition 6 directly extends to measures, functions and processes.

Frisch and Parisi (1985) and Halsey *et al.* (1986) interpreted $f(\alpha)$ as the fractal dimension of $T(\alpha) = \{t \in [0,T] : \alpha(t) = \alpha\}$, i.e. of the set of instants having local Hölder exponent $\alpha$. For various levels of the scale $\alpha$, Figure 1*d* illustrates the subintervals with coarse exponent $\alpha_k(t_i) > \alpha$. When the number of iterations $k$ is sufficiently large, these "cuts" display a self-similar structure. Appendix 8.5 provides a more detailed discussion of this interpretation.

### 4.2. The Spectrum of Multiplicative Measures

We now use Large Deviation Theory to compute the multifractal spectrum of multiplicative measures. First consider a *conservative* measure $\mu$ defined on the unit interval $[0,1]$. After $k$ iterations, we know the masses $\mu[t, t+\Delta t] = M(\eta_1)...M(\eta_1,..,\eta_k)$ in intervals of length $\Delta t = b^{-k}$. We can therefore calculate the coarse Hölder exponents

$$\begin{aligned} \alpha_k(t) &= \ln \mu[t, t+\Delta t] / \ln \Delta t \\ &= -\left[\log_b M(\eta_1) + ... + \log_b M(\eta_1,..,\eta_k)\right]/k. \end{aligned} \tag{4.2}$$

The multifractal spectrum is obtained by forming renormalized histograms of these exponents. It is therefore convenient to define $V_i \equiv -\log_b M(\eta_1,..,\eta_i)$ and interpret the coarse Hölder exponents as draws of the random variable

$$\alpha_k = \frac{1}{k}\sum_{i=1}^{k} V_i. \tag{4.3}$$

The spectrum $f(\alpha)$ can then be directly derived from the asymptotic distribution of $\alpha_k$. Since $\alpha_k$ is the average of $k$ iid random variables, its asymptotic distribution can be analyzed with the Strong Law of Large Numbers (SLLN) and Large Deviation Theory (LDT).

By the SLLN, $\alpha_k$ converges almost surely to[22]

$$\alpha_0 = \mathbb{E}\, V_1 = -\mathbb{E}\, \log_b M > 1. \tag{4.4}$$

[22] The relation $-\mathbb{E}\, \log_b M > 1$ follows from Jensen's inequality and $\mathbb{E}\, M = 1/b$.

As $k \to \infty$, almost all coarse exponents are contained in a small neighborhood of $\alpha_0$. The standard histogram $N_k(\alpha)/b^k$ thus collapses to a spike at $\alpha_0$ as anticipated in Section 4.1. The other coarse exponents do matter, and in fact, most of the mass concentrates on intervals with Hölder exponents that are bounded away from $\alpha_0$.[23] Information on these "rare events" is presumably contained in the tail of the random variable $\alpha_k$.

Tail behavior is the object of Large Deviation Theory. In 1938, H. Cramér established the following important theorem under conditions that were gradually weakened.

**Theorem 5.** *Let $\{X_k\}$ denote a sequence of iid random variables. Then as $k \to \infty$,*

$$\frac{1}{k} \ln \mathbb{P} \left\{ \frac{1}{k} \sum_{i=1}^{k} X_i > \alpha \right\} \to \inf_q \ln \left[ \mathbb{E}\, e^{q(\alpha - X_1)} \right],$$

*for any $\alpha > \mathbb{E}X_1$.*

Proofs of this theorem can be found in Billingsley (1979) and Durrett (1991).

Application of this theorem leads to

**Theorem 6.** *The multifractal spectrum $f(\alpha)$ is the Legendre transform*

$$f(\alpha) = \inf_q \left[ \alpha q - \tau(q) \right] \tag{4.5}$$

*of the scaling function $\tau(q)$.*

This result holds for both conservative and canonical measures, and the proof is sketched in the Appendix. The theorem provides the foundation of the empirical work developed in Section 6, where an estimation procedure for the scaling function $\tau(q)$ is obtained and the Legendre transform yields an estimate of the multifractal spectrum $f(\alpha)$.

Theorem 6 allows us to derive explicit formulae for the spectrum in a number of useful examples. To aid future reference, we denote by $f_\theta(\alpha)$ the spectrum

[23] Let $T_k$ denote the set of $b$-adic cells with local exponents greater than $(1 + \alpha_0)/2$. When $k$ is large, $T_k$ contains "almost all" cells, but its mass:

$$\sum_{t \in T_k} (\Delta t)^{\alpha_k(t)} \leq b^k (\Delta t)^{(\alpha_0+1)/2} = b^{-k(\alpha_0-1)/2}$$

vanishes as $k$ goes to infinity.

| **Distribution of $V$** | **Multifractal Spectrum $f_\theta(\alpha)$** |
|---|---|
| Normal$(\lambda, \sigma^2)$ | $1-(\alpha-\lambda)^2/[4(\lambda-1)]$ |
| Binomial | $-\frac{\alpha_{\max}-\alpha}{\alpha_{\max}-\alpha_{\min}}\log_2\left(\frac{\alpha_{\max}-\alpha}{\alpha_{\max}-\alpha_{\min}}\right)-\frac{\alpha-\alpha_{\min}}{\alpha_{\max}-\alpha_{\min}}\log_2\left(\frac{\alpha-\alpha_{\min}}{\alpha_{\max}-\alpha_{\min}}\right)$ |
| Poisson$(\gamma)$ | $1-\gamma/\ln b+\alpha\log_b(\gamma e/\alpha)$ |
| Gamma$(\beta,\gamma)$ | $1+\gamma\log_b(\alpha\beta/\gamma)+(\gamma-\alpha\beta)/\ln b$ |

Table 4.1: **Examples of Multifractal Spectra**
Using Large Deviation Theory, we can compute the Multifractal Spectrum of a multiplicative measure and its corresponding trading time when the random variable $V=-log_b M$ is respectively: (1) a Gaussian density of mean $\lambda$ and variance $\sigma^2$, (2) a binomial distribution with discrete values $\alpha_{min}$ and $\alpha_{max}$, (3) a discrete Poisson distribution $p(x)=e^{-\gamma}\gamma^x/x!$, and (4) a Gamma distribution with density $p(x)=\beta^\gamma x^{\gamma-1}e^{-\beta x}/\Gamma(\gamma)$.

common to a measure $\mu$ and its c.d.f. $\theta$. First consider a measure generated by a log-normal multiplier $M$ with distribution $-log_b M \sim \mathcal{N}(\lambda,\sigma^2)$. Conservation of mass imposes that $\mathbb{E}\,M=1/b$ or equivalently $\sigma^2=2\ln b/(\lambda-1)$. It is easy to show that the scaling function $\tau(q)\equiv-\log_b(\mathbb{E}\,M^q)-1$ has the closed-form expression $\tau(q)=\lambda q-1-q^2\sigma^2(\ln b)/2$. We infer from Theorem 6 that the multifractal spectrum is a quadratic function

$$f_\theta(\alpha)=1-(\alpha-\lambda)^2/[4(\lambda-1)]$$

parameterized by a unique number $\lambda>1$. Similarly, we can compute $f_\theta(\alpha)$ when the random variable $V$ is binomial, Poisson or Gamma (see CFM for detailed derivations). These results are reported in Table 2. We note that the spectrum is very sensitive to the distribution of the multiplier, which suggests that the MMAR has enough flexibility to model a wide range of financial prices. In the empirical work, this allows us to identify a multiplicative measure from its spectrum $f_\theta(\alpha)$, as implemented in Section 6.

### 4.3. Application to the MMAR

We now examine the spectrum of price processes generated by the MMAR. Denoting by $f_Z(\alpha)$ the spectrum of a process $Z(t)$, we show

**Theorem 7.** *The price $P(t)$ and the log-price $X(t)$ have identical multifractal spectra: $f_P(\alpha)\equiv f_X(\alpha)\equiv f_\theta(2\alpha)$.*

**Proof.** Given a process $Z$, denote $\alpha_Z(t)$ as its local scale at date $t$, and $T_Z(\alpha)$ as the set of instants with scale $\alpha$. At any date, the log-price has infinitesimal

variation

$$\begin{aligned} |X(t+\triangle t)-X(t)| &= |B[\theta(t+\triangle t)]-B[\theta(t)]| \\ &\sim |\theta(t+\triangle t)-\theta(t)|^{1/2} \\ &\sim |\triangle t|^{\alpha_\theta(t)/2}, \end{aligned}$$

and thus local scale $\alpha_X(t) \equiv \alpha_\theta(t)/2$. The sets $T_X(\alpha)$ and $T_\theta(2\alpha)$ coincide, and in particular have identical fractal dimensions: $f_X(\alpha) \equiv f_\theta(2\alpha)$. Moreover since the price $P(t)$ is a differentiable function of $X(t)$, the two processes have identical scales and spectra. ■

The log-price $X(t)$ contains a continuum of local exponents, and thus *cannot* be generated by an Itô diffusion process. Denote by $\alpha_0(Z)$ the most probable exponent of a process $Z$. At almost every instant, the log-price has a local scale $\alpha_0(X) \equiv \alpha_0(\theta)/2$ larger than $1/2$. Thus despite their irregularity, the MMAR's sample paths are almost everywhere smoother than the paths of a Brownian motion. Our analysis of Section 2 indicates that the variability of the MMAR is in fact explained by the "rare" local scales $\alpha < \alpha_0(X)$. While processes such as jump diffusions also permit zero Lebesgue measure sets to contribute to the total variation, it is notable that the MMAR has continuous paths with variations dominated by rare events.

The most probable exponent satisfies $\alpha_0(X) > 1/2$, and Theorem 1 implies that the standard deviation of the process

$$\sqrt{\mathbb{E}\left\{[X(t+\Delta t)-X(t)]^2\right\}} = c_X(2)^{1/2}\sqrt{\Delta t}$$

is of the order $(\Delta t)^{1/2}$. Thus while most shocks are of order $(\Delta t)^{\alpha_0(X)}$, the exponents $\alpha < \alpha_0(X)$ appear frequently enough to alter the scaling properties of the variance. This contrasts with the argument of standard textbooks,[24] where a

[24] Merton (1990, ch. 3) provides an interesting discussion of multiple local scales and "rare events" in financial processes. Assume that the price variation over a time interval $\Delta t$ is a discrete random variable taking values $\varepsilon_1, ..., \varepsilon_m$ with probability $p_1, .., p_m$, and assume moreover that $p_i \sim (\Delta t)^{q_i}$, $\varepsilon_i \sim (\Delta t)^{r_i}$ and $r_i > 0$ for all $i$. Denote by $I$ the events $i$ such that $p_i\varepsilon_i^2 \sim \Delta t$. When the variance of the process $\sum_{i=1}^m p_i\varepsilon_i^2$ is of the order $\Delta t$, only events in $I$ contribute to the variance. If all events belong to $I$, Merton establishes that only events of the order $(\Delta t)^{1/2}$ matter. The MMAR shows that events outside $I$ can play a crucial role in the statistical properties of the price process, a property previously overlooked in the literature.

standard deviation in $(\Delta t)^{1/2}$ implies that most shocks are of the same order. We expect these findings to have interesting consequences for decision and equilibrium theory.

Finally, long memory of the MMAR has a direct geometric interpretation. On a sample path, large variations are observed on the set of instants $LV = \{t : \alpha_X(t) < \alpha_0(X)\}$ where the local scale is smaller than the most probable exponent $\alpha_0(X)$. By Theorem 7, the set $LV$ has a positive fractal dimension and therefore clusters in certain regions of the time interval $[0, T]$. This explains the alternation of periods with large and small price changes. Furthermore, $LV$ is statistically self-similar since it has the same spreading of points as its subsets. Observing volatility in a given time period thus contains important information on future volatility.

## 5. An Extension with Autocorrelated Returns

The multifractal model presented in Section 3 is characterized by long memory in volatility but the absence of correlation in returns. Long memory has been identified in the first differences of many economic series, including aggregate output (Adelman, 1965; Diebold and Rudebusch, 1989; Sowell, 1992), the Beveridge (1925) Wheat Price Index, the US Consumer Price Index (Baillie, Chung and Tieslau, 1996), and interest rates (Backus and Zin, 1993).[25] This has lead authors to model these series with the fractional Brownian motion or the discrete time ARIMA specification. We note, however, that these economic series have volatility patterns which seem closer to the multifractal model than to the fractional Brownian motion. This suggests an extension of the MMAR which has both multifractal volatility and fractionally integrated increments.

The new model assumes that the economic series $X(t)$ is obtained by compounding a FBM with a multifractal trading time. Consistent with the notation of Section 3, we replace Assumption 1 by

**Assumption 1a.** *$X(t)$ is a compound process*

$$X(t) \equiv B_H[\theta(t)]$$

*where $B_H(t)$ is a Fractional Brownian motion, and $\theta(t)$ is a stochastic trading time.*

[25] Baillie (1996) provides a good review of this literature.

In addition, we maintain the multifractality of trading time (Assumption 2) and the independence of the processes $B_H(t)$ and $\theta(t)$ (Assumption 3). Note that the generalized model coincides with the MMAR if $H = 1/2$. For other values of the index $H$, the increments of $X(t)$ display either antipersistent ($H < 1/2$) or positive autocorrelations and long memory ($H > 1/2$). The more general model is fully developed in MFC, CFM, FCM and Mandelbrot (1997).

The self-similarity of $B_H(t)$ implies

**Theorem 8.** *The process $X(t)$ is a multifractal process with stationary increments, scaling function $\tau_X(q) = \tau_\theta(Hq)$, and multifractal spectrum $f_X(\alpha) = f_\theta(H\alpha)$.*

The proof of these results is provided in MFC. We observe that $\tau_X(1/H) = \tau_\theta(1) = 0$, which allows the estimation of the index $H$ in the empirical work. The generalized construction has scaling properties analogous to the MMAR, and provides a useful additional tool for empirical applications.

## 6. Empirical Evidence

### 6.1. Multifractal Moment Restrictions

Consider a price series $P(t)$ on the time interval $[0, T]$, and the log-price $X(t) \equiv \ln P(t) - \ln P(0)$. Partitioning $[0, T]$ into integer $N$ intervals of length $\triangle t$, we define the *sample sum* or *partition function*

$$S_q(T, \triangle t) \equiv \sum_{i=0}^{N-1} |X(i\triangle t + \triangle t) - X(i\triangle t)|^q \,. \tag{6.1}$$

When $X(t)$ is multifractal, the addends are identically distributed, and the scaling law (2.5) yields $\mathbb{E}[S_q\,(T, \triangle t)] = N c_X(q)(\triangle t)^{\tau_X(q)+1}$ when the $q^{th}$ moment exists. This implies

$$\ln \mathbb{E}[S_q(T, \triangle t)] = \tau_X(q) \ln(\triangle t) + c_X^*(q) \tag{6.2}$$

where $c_X^*(q) = \ln c_X(q) + \ln N$.

For each admissible $q$, equation (6.2) provides restrictions on how the partition function varies with increment size $\Delta t$. The possibility of rejecting these moment conditions in data provides a test of the multifractal model. Various methods may produce an estimate $\widehat{\tau}_X(q)$, which provides an estimate $\widehat{f}(\alpha)$ of the multifractal

spectrum through the Legendre transform (4.5). The spectrum is then mapped back into a distribution $M$ for multipliers in the cascade model of volatility, as suggested by Table 2.

The model permits both parametric and non-parametric estimation of $\tau_X(q)$. If we specify a parametric family of distributions for $M$, both $\widehat{\tau}_X(q)$ and $\widehat{f}(\alpha)$ are constrained to implied parametric families of functions, and these constraints can be imposed in estimation. Non-parametric estimation places few restrictions on the scaling function and the multifractal spectrum. Since $\tau_\theta(q) = -\log_b \mathbb{E}(M^q) - 1$, the scaling function provides all the finite moments of $M$. While this does not always uniquely identify the distribution of $M$, it is nonetheless informative.[26]

This paper uses a very simple approach to testing and estimation. For a set of positive $q$, and a set of time scales $\Delta t$, we calculate the partition functions $S_q(T, \triangle t)$ of the data. The partition functions are then plotted against $\Delta t$ in logarithmic scales. By (6.2), the multifractal model implies that these plots should be approximately linear when the $q^{th}$ moment exists. If this condition holds, OLS estimates of the slopes provide the corresponding scaling exponents $\widehat{\tau}_X(q)$.[27]

An advantage of this procedure is its transparency. Plotting the sample sums provides striking visual evidence of moment scaling, a new empirical regularity that will be useful in modelling many financial data sets. We anticipate, however, several extensions to this methodology as the literature progresses. First, note that the moment restrictions in (6.2) may be highly correlated across different $q$ and $\Delta t$, suggesting a Generalized Method of Moments (GMM) approach.[28] Whereas the plotting methodology produces a series of graphs that are inspected for linearity for each $q$, GMM could provide a single test statistic for an arbitrary set of the moment restrictions. Additionally, GMM provides standard errors and increases efficiency by permitting joint estimation of the scaling exponents $\tau(q)$.

Because of the limitations of our current methodology, we conduct simulation experiments designed to test the estimation method itself. The plotting methodology is first applied to simulated samples from the estimated multifractal data generating process. We then simulate estimated GARCH and FIGARCH alter-

[26] Feller (1971), Durrett (1991) and Mandelbrot (1997) provide good discussions of the uniqueness problem in moments.

[27] In the data, using weighted least squares produces very similar results since the plots are approximately linear.

[28] Analytical calculation of the covariance matrix of moment restrictions is non-trivial. However, one could use a two-step methodology that employs a consistent estimator for $\tau(q)$ in the first stage. The covariance matrix of moment restrictions can then be estimated by simulating the inferred process, and used in the second stage.

natives and examine whether these reproduce the scaling properties of the data.

### 6.2. Deutschemark / US Dollar Exchange Rates

We first investigate multifractality of Deutschemark / US Dollar ("DM/USD") exchange rates. We use two data sets provided by Olsen and Associates, a currency research and trading firm based in Zürich. The first data set ("daily") consists of a twenty four year series of daily data spanning June 1973 to December 1996. Olsen collects price quotes from banks and other institutions through several electronic networks. A price quote is converted to a single *price observation* by taking the geometric mean of the concurrent bid and ask. The reported price in the daily data is then calculated by linear interpolation of the price observations closest to 16:00 UK on each side.[29] Figure 3 shows the daily data, which exhibits volatility clustering at all time scales and intermittent large fluctuations.

The second data set ("high-frequency") contains all bid/ask quotes and transmittal times collected over the one year period from October 31, 1992 to September 1, 1993. We convert quotes to price observations using the same methodology as Olsen. This provides a round-the-clock data set of $1,472,241$ observations. Olsen provides a flag for quotes believed to be erroneous or not representative of actual willingness to trade. We eliminate these observations, which constitute 0.36% of the dataset. Combining the daily data and the high-frequency data allows us to calculate partition functions over three orders of magnitude for $\triangle t$.

The high-frequency data show strong patterns of daily seasonality. In continuous time, seasonality is a smooth transformation that does not affect local Hölder exponents. However since our data set is discrete, we may expect seasonality to introduce noise. To reduce this effect, we can write a seasonally modified version of the MMAR:

$$\ln P(t) - \ln P(0) = B_H \left\{ \theta \left[ SEAS(t) \right] \right\},$$

where the seasonal transformation $SEAS(t)$ is a differentiable function of clock time. In this paper, we use a prefilter that smoothes variation in average absolute returns over fifteen minute intervals of the week. An earlier working paper (FCM) provides details on this and three other seasonal prefilters, and finds small, predictable differences in results depending on the deseasonalizing method. Moreover, except for the reduction in noise, there are no systematic differences in reported results for filtered and unfiltered data.

[29] An earlier working paper (FCM) also uses noon buying rates provided by the Federal Reserve, and finds no significant difference in reported results.

### 6.3. Main Results

We first calculate partition functions for each of the two DM/USD data sets. Increments $\Delta t$ range from fifteen seconds to two weeks in the high frequency data, and from one day to six months in the daily data. Values of $\Delta t$ are chosen to increase multiplicatively by a factor of 1.1 from minimum to maximum. For different ranges of $q$ and $\Delta t$, Figures 4 and 5 show renormalized plots of the partition function against $\Delta t$ in logarithmic scales. Since we focus on the slopes $\widehat{\tau}_X(q)$ but not the intercepts, plots for each $q$ are renormalized by vertical displacement to begin at zero for the lowest value of $\Delta t$ in each graph. This allows plots for many $q$ to be presented simultaneously. The daily and high frequency plots are presented in the same graph to highlight the similarity in their slopes. This is achieved by a second vertical displacement of the daily data that provides the best linear fit.[30]

Figure 4 shows the full range of calculated $\Delta t$, from fifteen seconds to six months, and five values of $q$ ranging from 1.75 to 2.25. This range of $q$ permits estimation of the self-affinity index $H$ in the extended model presented in Section 5. Since $\tau_X(1/H) = 0$ and the standard Brownian specification $H = 1/2$ has previous empirical support, we expect to find $\tau_X(q) = 0$ for a value of $q$ near two.

We first note the approximate linearity of the partition functions beginning at $\Delta t = 1.4$ hours and extending to the largest increment used, $\Delta t = 6$ months. In this range, the slope is zero for a value of $q$ slightly smaller than two, and we report

$$\widehat{H} \approx .53,$$

which implies very slight persistence in the DM/USD series. We do not estimate standard errors, but this result is sufficiently close to $H = 1/2$ to appear consistent with the martingale hypothesis for returns.

The two breaks in the linearity of the partition functions in Figure 4 are evidence that the standard multifractal model breaks down at high frequencies, and are thus called *high-frequency crossovers*. These crossovers presumably relate to market frictions such as bid-ask spreads, discreteness of quoting units, and discontinuous trading. These frictions become increasingly important relative to price variation as the time scale decreases. In particular, the average spread is 0.07 pfennig,[31] while the absolute change in the exchange rate averages 0.14 pfennig

[30] The linear fit is performed using OLS under the restriction that both lines have the same slope.

[31] One pfennig equals 0.01 $DM$. The two most common spread sizes are 0.05 pfennig (38.25%), and 0.10 pfennig (52.55%), together comprising over 90% of all observed spreads.

over a time increment of $\Delta t = 1.4$ hours, which corresponds to the first high-frequency crossover. Since the spread has the same order of magnitude as the price variation, it is not surprising that market microstructure begins to affect scaling at this time scale.[32] From the evidence in Figure 4, we thus identify moment scaling in the DM/USD data that begins at $\Delta t = 1.4$ hours and extends at least to the maximum value considered of $\Delta t = 6$ months.

Figure 5 presents partition functions for a larger range of moments $1.5 \leq q \leq 5$ for the scaling range $\Delta t \geq 1.4$ hours. Larger moments capture information in the tails of the distribution of returns, and are thus generally more sensitive to deviations from scaling. All plots are remarkably linear, and the overlapping values from the two data sets have almost the same slope.[33] Thus despite the apparent non-stationarity of the 24 year series – such as long price swings and long cycles of volatility – the moment restrictions imposed by the MMAR seem to hold over a broad range of sampling frequencies. Extracting the estimated slopes from these plots and additional moments $q$, Figure 6 presents estimated scaling functions $\widehat{\tau}_X(q)$ for both data sets. The estimated scaling functions are strictly concave, indicating multifractality, and are fairly similar except for very large moments which produce greater estimation error.

As suggested by Theorem 6, the estimated multifractal spectrum $\widehat{f}_X(\alpha)$ is given by the Legendre transform of $\widehat{\tau}_X(q)$. Figure 7 shows the estimated multifractal spectrum of the daily data.[34] The estimated spectrum is concave, in contrast to the degenerate spectra of Brownian Motion and other unifractals. Using the estimated spectrum, we can recover a generating mechanism for trading time based upon the canonical multiplicative cascades described in Section 2.2.

The spectrum of daily data is very nearly quadratic. Section 4.2 shows that quadratic spectra are generated by lognormally distributed multipliers $M$. We thus specify $-\log_b M \sim \mathcal{N}(\lambda, \sigma^2)$, giving trading time $\theta(t)$ with multifractal spectrum $f_\theta(\alpha) = 1 - (\alpha - \lambda)^2/[4(\lambda - 1)]$. The log-price process has most probable

[32] Moreover, for time scales between 3.6 minutes and 1.4 hours, the partition function has approximate slope of zero for the moment $q = 2.25$. This implies $H$ near 0.44 and negative autocorrelation at high frequencies, which further supports a bid-ask spread explanation for the crossover.

[33] We also observe an apparent increase in variability with the time scale $\Delta t$, which can be attributed to the shrinking number of addends in the partition function at low frequencies. Because the plots are approximately linear, accounting for differences in variability through weighted least squares has little effect on the reported results.

[34] The estimated multifractal spectrum of the high frequency data is similar in many respects, and is discussed in FCM.

exponent $\alpha_0 = \lambda H$, and spectrum

$$f_X(\alpha) = 1 - \frac{(\alpha - \alpha_0)^2}{4H(\alpha_0 - H)}$$

Since $\widehat{H} = 0.53$, the single free parameter $\alpha_0$ is used to fit the estimated spectrum. We report

$$\widehat{\alpha_0} = .589,$$

which produces the parabola shown in Figure 8. Choosing a generating construction with base $b = 2$, this immediately implies $\widehat{\lambda} = 1.11$, $\widehat{\sigma}^2 = 0.32$.

The estimated value of the most probable local Hölder exponent $\alpha_0$ is greater than 1/2. On a set of Lebesgue measure 1, the estimated multifractal process is therefore more regular than a Brownian Motion. However, the concavity of the spectrum also implies the existence of lower Hölder exponents that correspond to more irregular instants of the price process. These contribute disproportionately to volatility.[35]

### 6.4. Monte Carlo Simulations

We now present simulation experiments designed to provide a preliminary assessment of our estimation procedure. One first would like to determine whether the inferred multifractal generating mechanism does in fact reproduce the scaling properties in the data. This requires simulating the estimated multifractal process, and applying the plotting methodology to the simulated data. Figure 8 shows raw simulated data and log differences of the estimated process. The simulated sample shows a variety of large price changes, apparent trends, persistent bursts of volatility, and other characteristics found in the USD/DM data.

Figure 9*a* shows the partition function plots of four random simulations. The plots are approximately linear and tend to follow their theoretically predicted slopes, which are nearly identical to the slopes estimated in the DM/USD data. Repetition of this exercise can provide a more thorough assessment of the estimation method. Preliminary work indicates that estimated slopes have small biases that become small as sample size grows, but also a relatively large degree

[35] Moreover, because of the particular structure of fractal sets, the set of instants with a particular value of $\alpha$ tends to be clumped together, simultaneously generating more risk and long memory in volatility. See Appendix 8.6 for further discussion on fractal clustering of local scales.

of estimation error in typical sample sizes.[36] Since a thorough analysis of these econometric issues is relatively complex, and may be made obsolete by the development of an appropriate GMM methodology, we leave these topics for future research. From the preliminary results in Figure 9*a*, we observe that the multifractal model can replicate the scaling features of the data. The simple plotting methodology also appears to be a useful first step in designing estimators for multifractal processes.

Another important question is whether other standard econometric models possess scaling properties. To assess this, we apply the plotting methodology to simulated GARCH and FIGARCH processes with parameters taken from previously published research on daily DM/USD exchange rates. Figure 9*b* shows four simulated partition functions from a GARCH$(1,1)$ process with parameter values taken from Baillie and Bollerslev (1989). Figure 9*c* shows simulated partition functions from the preferred FIGARCH$(1,d,0)$ specification estimated in Baillie, Bollerslev, and Mikkelsen (1996). The simulated GARCH partition functions appear fairly linear, but their apparent slope is similar to the predicted slope of Brownian Motion rather than the data. This is symptomatic of the fact that GARCH models are short memory processes. Over long time periods, temporal clustering disappears, and thus GARCH should be expected to scale like Brownian Motion at low frequencies. For low values of $\Delta t$, the GARCH partition functions increase more quickly than Brownian Motion, indicating the effect of volatility clustering. But this effect disappears as $\Delta t$ grows. Because FIGARCH contains long-memory in volatility, it may behave differently at low frequencies than the Brownian Motion. However, the FIGARCH partition functions tend to be more irregular than both the MMAR partition functions and the data, and do not often have the same slopes as the data. While statistical testing against the various alternatives requires further econometric research, the simple plotting methodology does appear to discriminate between competing models.

### 6.5. Equity Data

After observing multifractal properties in DM/USD exchange rates, it is natural to test the model on other financial data. This section presents evidence of moment-

[36] Another interesting finding is that at comparable sample sizes, simulated partition functions tend to show more variability around their slope than we find in the data. This suggests stronger scaling in the data than in the estimated multifractal process, which is somewhat surprising since the model has been designed to capture scaling. It is difficult to distinguish, however, whether this should be attributed to the model or bias in the estimation method.

scaling in a sample of five major U.S. stocks and one equity index.[37]

The Center for Research in Security Prices ("CRSP") provides daily stock returns for 9,190 trading days from July 1962 to December 1998. We present results for the value weighted NYSE-AMEX-NASDAQ index[38] ("CRSP Index") and five stocks: Archer Daniels Midland ("ADM"), General Motors ("GM"), Lockheed-Martin ("Lockheed"), Motorola, and United Airlines ("UAL"). The individual stocks are issued by large, well-known corporations from various economic sectors, and have reported data for the full CRSP sample span.[39] For each series, we convert the daily return data into a renormalized log-price series $X_t$, and then apply the partition function methodology described in Section 6.2.[40]

Figure 10 shows results for the CRSP index and GM. In the first two panels, the full data sets are used with increments $\Delta t$ ranging from one day to approximately one year. The partition functions for moments $q = \{1, 2, 3\}$ are approximately linear for both series, with little variation around the apparent slope.[41] In contrast, the partition functions vary considerably for $q = 5$, making a determination of linearity in their expectations more difficult. This suggests investigation of the tails of the data. We find that the behavior of the fifth moment is dominated by volatility surrounding the stock market crash of October 1987. This is demonstrated by the second two panels of Figure 10, which show striking linearity after simply removing the crash day from both data sets.

Since discarding data is an unsatisfactory approach to financial modelling,[42]

[37] The multifractal model offers a flexible framework that may be amenable to many types of financial prices, but the version presented in this paper is not intended to be applied directly to equities. In contrast to exchange rates, equities require further consideration of mean returns. For example, one might permit negative correlation between the Brownian Motion $B$ and the trading time $\theta(t)$ to account for conditional skewness. In the absence of an explicit model, the empirical work in this section investigates scaling in raw returns.

[38] The index return on each day is calculated as the value weighted average return including cash distributions for all stocks from the NYSE, AMEX, and NASDAQ exchanges with reported return data for the day. Weights are given by market capitalization on the previous day.

[39] Choosing stocks with full samples allows testing of the moment-scaling restrictions over a larger range of frequencies.

[40] The CRSP holding period returns $r_t = [P_t - P_{t-1} + d_t]/P_{t-1}$ include cash distributions $d_t$. We construct the series $\{X_t\}_{t=0}^{T}$ by $X_0 = 0$, $X_t = X_{t-1} + \ln(1 + r_t)$.

[41] The CRSP Index has noticeably positive slope for the moment $q = 2$, which indicates persistence. This characteristic is very atypical of individual securities.

[42] While discarding data may be justified in specific circumstances, our approach in this paper has been to build a stationary model flexible enough to accomodate a wide range of changing economic circumstances. This includes both long-range structural shifts, and extreme tail events such as the 1987 crash.

we reexamine the full data sets. The partition functions $S_{q=5}(T, \Delta t)$ for both series drop considerably from $\Delta t = 2$ days to $\Delta t = 3$ days. In the raw data, the CRSP index falls 17% on the day of the crash, but rebounds more than 8% two days later. GM loses 21% in the crash, recovering almost all its losses over the next two days. When $\Delta t = 3$ days, aggregation of these returns within a single interval contributes to the severe declines in the $q = 5$ partition functions.[43] As $\Delta t$ grows, the crash and the two following days occasionally fall in separate intervals and the partition functions spike.[44] More often, however, these three days lie within a single interval when $\Delta t$ is large.

The partition functions $S_5(T, \Delta t)$ for the full data sets thus show large variability for low $\Delta t$, and estimates of their slopes would appear to be relatively imprecise. After removing the crash from both data sets, the same partition functions appear to give a more precise fit, but at a cost. Both slopes increase to appear more Brownian or "mild," suggesting that important information has been lost. Additionally, removing the crash does not necessarily improve fit since our moment restrictions constrain only the expectations of the partition functions, not their variability.[45] Thus, the artifice of removing the crash (or similarly trimming the data) gives a false impression of improved model fit and alters scaling properties to imply a much milder process.

In contrast to GM and the CRSP index, the other four stocks in our sample scale remarkably well despite the crash.[46] These results are shown in Figure 11. Consistent with the martingale hypothesis for returns, three of the four stocks

[43] When calculating the partition functions for $\Delta t = 2$ days, the crash day and the two following days belong to separate intervals, each of which make large contributions to $S_5(T, \Delta t = 2$ days). When $\Delta t = 3$ days, however, the crash and the two following days belong to a single interval. Their returns partially cancel when aggregated, explaining the decreases in the partition functions $S_5(T, \Delta t)$ at $\Delta t = 3$ days.

[44] Additionally, the size of these spikes decreases with $\Delta t$ because of the diminishing influence of the crash on high sample moments. Together with the decreasing frequency of crash-related spikes in the partition functions, this explains why both plots of $S_5(T, \Delta t)$ become less variable as $\Delta t$ increases. In most cases, we expect partition function variability to increase with $\Delta t$ because moments must be calculated with fewer observations. For GM and the CRSP index, however, sharp rebounds from the crash cause larger variation at high frequencies.

[45] Incorporating moment restrictions that reflect the variability of the partition function plots is a promising avenue for future research.

[46] Extreme sensitivity to the crash in the $q = 5$ partition function seems to concentrate in the very largest stocks. Results for IBM, ATT, Kodak, Coca-Cola, Exxon, P&G, Sears, 3M, and a few other similar large stocks tend to look like the results for GM and the CRSP Index. This pattern is not as apparent for even marginally smaller stocks.

have almost exactly flat partition functions for $q = 2$, while ADM has a slight negative slope. The difference between Brownian scaling and multiscaling becomes perceptible for $q = 3$, and for the fifth moment, this difference is pronounced. UAL appears the most variable, with lower slopes at higher moments and thus a wider multifractal spectrum.

While not exhaustive, this analysis indicates that moment-scaling is a prominent feature of many equity series. We anticipate the confirmation of scaling in additional financial data, and suggest that future work consider not just the existence of scaling, but also its range of behaviors. Some data may appear closer to Brownian than the examples studied here, while others will appear more "wild." The most interesting extensions may investigate whether scaling behaviors can lead to economic insights. For example, we observed that anomalous scaling in high moments due to the 1987 crash tends to concentrate among the very largest firms in the CRSP database. We also observed that the CRSP index scales very differently in its second moment than individual securities.[47] While these findings are preliminary, they suggest that the partition function plots summarize a great deal of information in a convenient form. Analysis of moment-scaling may thus be useful in uncovering empirical regularities, and in evaluating and building financial models.

## 7. Conclusion

This paper investigates the multifractal model of asset returns, a continuous time stochastic process that incorporates the outliers and volatility persistence exhibited by many financial time series. The model compounds a standard Brownian Motion with an independent multifractal time-deformation process that produces volatility clustering. We show how to construct a class of candidate time-deformation processes as the limit of a simple iterative procedure, called a multiplicative cascade. The cascade provides parsimonious modelling, and results in a generalized scaling rule that restricts return moments to vary as power laws of the time increment. The price process is a semi-martingale with uncorrelated returns, and thus precludes arbitrage in a standard two-asset setting.

[47] The scaling of the second moment of the CRSP index indicates persistence. Previous work, for example Boudoukh, Richardson, and Whitelaw (1994), focuses on the persistence of portfolio returns at short horizons. The atypical scaling of the CRSP index, however, appears to be present at horizons as long as one year.

The MMAR introduces a fundamentally new class of processes to both finance and mathematics. Multifractal processes have continuous sample paths, but lie outside the class of Itô diffusions. Whereas standard processes can be characterized by a single local scale that describes the local growth rate of variation, sample paths of multifractal processes contain a *continuum* of local Hölder exponents within any time interval. The distribution of these exponents is conveniently quantified by a renormalized density, the multifractal spectrum $f(\alpha)$. For a large class of multifractal processes, the spectrum can be explicitly derived from Cramér's Large Deviation Theory. We demonstrate through a number of examples the sensitivity of the multifractal spectrum to the generating mechanism. The applied researcher may thus relate an empirical estimate of the spectrum back to a particular construction of the process, and is permitted considerable flexibility in modelling different types of data.

We find evidence of multifractality in the moment-scaling behavior of Deutschemark / US Dollar exchange rates. Over a range of observational frequencies from approximately two hours to 180 days, and over a range of time from 1973 to 1996, moments of the data grow approximately like a power law. We obtain an estimate of the multifractal spectrum by a Legendre transform of the moments' growth rates. From the shape of the estimated spectrum, we infer a lognormal distribution as the primitive of the generating mechanism, and estimate its parameters. We simulate the process, and confirm that the multifractal model replicates the moment behavior found in the data. We also demonstrate scaling behavior in an equity index and five major U.S. stocks.

The results of this paper indicate several directions for future research. We anticipate improvements in the empirical methodology through systematic Monte Carlo simulations and econometric theory based on the Generalized Method of Moments. Risk analysis, forecasting, and option pricing are promising applications developed in other papers. Further research will seek to derive the MMAR as an equilibrium process of economies with fully rational agents. In such frameworks, multifractality is expected to arise in equilibrium either exogenously, for instance as a consequence of multifractal technological shocks, or endogenously because of market incompleteness or informational cascades. The early empirical success of the MMAR thus offers new challenges in econometrics, finance, and economic theory.

# 8. Appendix

## 8.1. Scaling Rule

This Appendix analyzes the set $\mathcal{D}$ defined by a multiplicative measure with parameter $b \geq 2$. Consider a fixed instant $t \in [0,1]$. For all $\varepsilon > 0$, there exists a dyadic number $t_n$ such that $|t_n - t| < \varepsilon$. We can then find a number $\Delta_n = b^{-k_n} < \varepsilon$ for which $(t_n, \Delta_n) \in \mathcal{D}$. In the plane $\mathbb{R}^2$, the point $(t, 0)$ is thus the limit of the sequence $(t_n, \Delta_n) \in \mathcal{D}$, which establishes

**Property 1.** *The closure of $\mathcal{D}$ contains the set $[0,1] \times \{0\}$.*

The scaling relation (2.4) thus holds "in the neighborhood of any instant".

## 8.2. Proof of Proposition 1

Consider two exponents $q_1, q_2$, and two positive weights $w_1, w_2$ adding up to one. Hölder's inequality implies

$$\mathbb{E}\left(|X(t)|^q\right) \leq \left[\mathbb{E}\left(|X(t)|^{q_1}\right)\right]^{w_1} \left[\mathbb{E}\left(|X(t)|^{q_2}\right)\right]^{w_2},$$

where $q = w_1 q_1 + w_2 q_2$. Taking logarithms and using (2.5), we obtain

$$\ln c(q) + \tau(q) \ln t \leq [w_1 \tau(q_1) + w_2 \tau(q_2)] \ln t + [w_1 \ln c(q_1) + w_2 \ln c(q_2)]. \quad (8.1)$$

We divide by $\ln t < 0$, and let $t$ go to zero:

$$\tau(q) \geq w_1 \tau(q_1) + w_2 \tau(q_2), \quad (8.2)$$

which establishes the concavity of $\tau$. In fact this proof contains additional information on multifractal processes. Assuming that relation (2.5) holds for $t \in [0, \infty)$, we divide inequality (8.1) by $\ln t > 0$ and let $t$ go to infinity. We obtain the reverse of inequality (8.2), and conclude that $\tau(q)$ is linear. Thus multiscaling can only hold for *bounded* time intervals $\mathcal{T}$.

## 8.3. Proof of Theorem 1

Since the trading time and the Brownian motion $B(t)$ are independent, conditioning on $\theta(t)$ yields

$$\begin{aligned} \mathbb{E}\left\{|X(t)|^q \mid \theta(t) = u\right\} &= \mathbb{E}\left[\,|B(u)|^q \mid \theta(t) = u\,\right] \\ &= \theta(t)^{q/2}\, \mathbb{E}\left[|B(1)|^q\right], \end{aligned}$$

and thus $\mathbb{E}\left[|X(t)|^q\right] = \mathbb{E}\left[\theta(t)^{q/2}\right]\, \mathbb{E}\left[|B(1)|^q\right]$. The process $X(t)$ satisfies the multiscaling relation (2.5), with $\tau_X(q) \equiv \tau_\theta(q/2)$ and $c_X(q) \equiv c_\theta(q/2)\, \mathbb{E}\left[|B(1)|^q\right]$.

### 8.4. Proof of Theorem 2

Let $\mathcal{F}_t$ and $\mathcal{F}'_t$ denote the natural filtrations of $\{X(t)\}$ and $\{X(t), \theta(t)\}$. For any $t, T, u$, the independence of $B$ and $\theta$ implies

$$\begin{aligned} \mathbb{E}\{\, X(t+T) \mid \mathcal{F}'_t, \theta(t+T) = u \,\} &= \mathbb{E}\{\, B(u) \mid \mathcal{F}'_t \,\} \\ &= B[\theta(t)], \end{aligned}$$

since $\{B(t)\}$ is a martingale. We now infer that $\mathbb{E}[\, X(t+T) \mid \mathcal{F}_t\,] = X(t)$, which establishes that $X(t)$ is a martingale and has thus uncorrelated increments. The price $P(t)$ is a smooth function of $X(t)$ and therefore a semi-martingale, which precludes arbitrage opportunities in the two asset economy.

### 8.5. Proof of Theorem 4

**1. Trading Time**

Consider a canonical cascade after $k \geq 1$ stages. Consistent with the notation of Section 2, the interval $[0, T]$ is partitioned into cells of length $\Delta t = b^{-k}T$, and $I_1 = [t_1, t_1 + \Delta t]$ and $I_2 = [t_2, t_2 + \Delta t]$ denote two distinct cells. Assume that the first $l \geq 1$ terms are equal in the $b$-adic expansions of $t_1/T$ and $t_2/T$, so that $t_1/T = 0.\eta_1..\eta_l\eta_{l+1}..\eta_k$ and $t_2/T = 0.\eta_1..\eta_l\eta'_{l+1}..\eta'_k$, with $\eta'_{l+1} \neq \eta_{l+1}$. The distance $t = |t_2 - t_1|$ satisfies $b^{-l-1} \leq t/T < b^{-l}$, and the product $\mu(I_1)^q\mu(I_2)^q$, which is equal to

$$\begin{aligned} &\Omega(\eta_1, .., \eta_k)^q\, \Omega(\eta'_1, .., \eta'_k)^q\, M(\eta_1)^{2q}..M(\eta_1, .., \eta_l)^{2q} \\ &M(\eta_1, .., \eta_{l+1})^q..M(\eta_1, .., \eta_k)^q\, M(\eta'_1, .., \eta'_{l+1})^q..M(\eta'_1, .., \eta'_k)^q, \end{aligned}$$

has mean $(\mathbb{E}\Omega^q)^2[\mathbb{E}M^{2q}]^l[\mathbb{E}M^q]^{2(k-l)}$. We conclude that

$$\begin{aligned} Cov[\mu(I_1)^q; \mu(I_2)^q] &= (\mathbb{E}\Omega^q)^2(\mathbb{E}M^q)^{2k}\left\{[(\mathbb{E}M^{2q})/(\mathbb{E}M^q)^2]^l - 1\right\} \\ &= C_1(\Delta t)^{2\tau_\theta(q)+2}\left[b^{-l[\tau_\theta(2q)-2\tau_\theta(q)-1]} - 1\right] \end{aligned}$$

is bounded by two hyperbolic functions of $t$.

**2. Log-Price**

Since $B(t)$ and $\theta(t)$ are independent processes, the conditional expectation

$$\mathbb{E}\{\,|X(0,\Delta t)X(t,\Delta t)|^q|\,\theta(\Delta t)=u_1,\theta(t)=u_2,\theta(t+\Delta t)=u_3\}\,, \tag{8.3}$$

simplifies to

$$\mathbb{E}[\,|B(u_1)|^q]\;\mathbb{E}[\,|B(u_3)-B(u_2)|^q]=|u_1|^{q/2}\;|u_3-u_2|^{q/2}\;[\mathbb{E}|B(1)|^q]^2\,.$$

Taking expectations, we infer that

$$\mathbb{E}[\,|X(0,\Delta t)X(t,\Delta t)|^q\,]=\mathbb{E}\Big[\,|\theta(0,\Delta t)\theta(t,\Delta t)|^{q/2}\,\Big]\;[\,\mathbb{E}|B(1)|^q\,]^2$$

and therefore $\delta_X(t,q)=\delta_\theta(t,q/2)\;[\mathbb{E}|B(1)|^q]^2\,.$

### 8.6. Interpretation of $f(\alpha)$ as a Fractal Dimension

Fractal geometry considers irregular and winding structures that are not well described by their Euclidean length. For instance, a geographer measuring the length of a coastline will find very different results as she increases the precision of her measurement. In fact, the structure of the coastline is usually so intricate that the measured length diverges to infinity as the geographer's measurement scale goes to zero. For this reason, we cannot use the Euclidean length to compare two different coastlines, and it is natural to introduce a new concept of dimension. Given a precision level $\varepsilon>0$, we consider coverings of the coastline with balls of diameter $\varepsilon$. Let $N(\varepsilon)$ denote the smallest number of balls required for such a covering. The approximate length of the coastline is defined by $L(\varepsilon)=\varepsilon N(\varepsilon)$. In many cases, $N(\varepsilon)$ satisfies a power law as $\varepsilon$ goes to zero:

$$N(\varepsilon)\sim\varepsilon^{-D},$$

where $D$ is a constant called the *fractal* or *Hausdorff-Besicovitch dimension*. Fractal dimension helps to analyze the structure of a fixed multifractal. For any $\alpha\geq 0$, we can define the set $T(\alpha)$ of instants with Hölder exponent $\alpha$. As any subset of the real line, $T(\alpha)$ has a fractal dimension $D(\alpha)$, which satisfies $0\leq D(\alpha)\leq 1$. It can be shown that for a large class of multifractals, the dimension $D(\alpha)$ coincides with the multifractal spectrum $f(\alpha)$.

In the case of measures, we can provide a heuristic interpretation of this result based on coarse Hölder exponents. Denoting by $N(\alpha,\Delta t)$ the number of intervals $[t,t+\Delta t]$ required to cover $T(\alpha)$, we infer from Equation (4.1) that: $N(\alpha,\Delta t)\sim$

$(\Delta t)^{-f(\alpha)}$. We then rewrite the total mass $\mu[0,T] = \sum \mu(\Delta t) \sim \sum (\Delta t)^{\alpha(t)}$, and rearrange it as a sum over Hölder exponents:

$$\mu[0,T] \sim \int (\Delta t)^{\alpha - f(\alpha)}\, d\alpha.$$

The integral is dominated by the contribution of the Hölder exponent $\alpha_1$ that minimizes $\alpha - f(\alpha)$, and therefore

$$\mu[0,T] \sim (\Delta t)^{\alpha_1 - f(\alpha_1)}$$

Since the total mass $\mu[0,T]$ is positive, we infer that $f(\alpha_1) = \alpha_1$, and $f(\alpha) \leq \alpha$ for all $\alpha$. When $f$ is differentiable, the coefficient $\alpha_1$ also satisfies $f'(\alpha_1) = 1$. The spectrum $f(\alpha)$ then lies under the $45^o$ line, with tangential contact at $\alpha = \alpha_1$.

### 8.7. Large Deviation Theory and the Multifractal Spectrum

This Appendix sketches the proof of Theorem 6, and introduces the concepts of latent and virtual Hölder exponents.[48] First consider a *conservative* multiplicative measure $\mu$. Application of LDT begins with the histogram method of Section 4.1: Subdivide the range of $\alpha$s into intervals of length $\Delta\alpha$, and denote by $N_k(\alpha)$ the number of coarse Hölder exponents in the interval $(\alpha, \alpha + \Delta\alpha]$. For large values of $k$, we write

$$\frac{1}{k} \log_b \left[ \frac{N_k(\alpha)}{b^k} \right] \sim \frac{1}{k} \log_b \mathbb{P}\left\{ \alpha < \alpha_k \leq \alpha + \Delta\alpha \right\}. \tag{8.4}$$

This relation holds exactly for multinomial measures, which have discrete coarse exponents $\alpha_k$, but is postulated in more general cases. For any $\alpha > \alpha_0$, Cramér's theorem implies

$$k^{-1} \log_b \mathbb{P}\left\{ \alpha_k > \alpha \right\} \to \inf_q \log_b \left[ \mathbb{E}\, e^{q(\alpha - V_1) \ln b} \right] \tag{8.5}$$

as $k \to \infty$. Using the definition of the scaling function, we simplify the limit to $\inf_q [\alpha q - \tau(q)] - 1$. Combining this with (4.1) and (8.4), it follows[49] that Theorem 6 holds.

[48] We refer the reader to Mandelbrot (1989b), Peyrière (1991) and CFM for more detailed discussions.

[49] See CFM for a more detailed proof.

These arguments easily extend to a *canonical* measure $\mu$. Given a $b$-adic instant $t$, the coarse exponent $\alpha_k(t) = \ln \mu[t, t+\Delta t]/\ln \Delta t$ is the sum of a high frequency component, $-\log_b \Omega(\eta_1, ..., \eta_k)/k$, and of the familiar low frequency average

$$\alpha_{k,L}(t) = -\left[\log_b M(\eta_1) + ... + \log_b M(\eta_1, .., \eta_k)\right]/k.$$

The exponent $\alpha_k(t)$ converges almost surely to $\alpha_0 = -\mathbb{E}\log_b M$, and the multifractal spectrum is again the Legendre transform of the scaling function $\tau(q)$.

Relation (8.5) also shows that $f(\alpha)$ is the limit of

$$\begin{array}{lll} k^{-1}\log_b \mathbb{P}\{\alpha_{k,L}(t) > \alpha\} + 1 & \text{if } \alpha > \alpha_0, & \text{and} \\ k^{-1}\log_b \mathbb{P}\{\alpha_{k,L}(t) < \alpha\} + 1 & \text{if } \alpha < \alpha_0. & \end{array}$$

$f(\alpha)$ is therefore a hump-shaped function, reaching a maximum at the most probable exponent: $f(\alpha) \leq f(\alpha_0) = 1$.[50] We have successively viewed the spectrum $f(\alpha)$ as:

(D1) the limit of a renormalized histogram of coarse Hölder exponents,

(D2) the fractal dimension of the set of instants with Hölder exponent $\alpha$,

(D3) the limit of $k^{-1}\log_b \mathbb{P}\{\alpha_{k,L}(t) > \alpha\} + 1$ provided by LDT.

The three definitions coincide for multinomial measures, and $(D1)$ and $(D2)$ agree for a large class of multifractals (Peyrière, 1991). However, $(D1)$ and $(D2)$ imply that $f(\alpha) \geq 0$, while $(D3)$ imposes no such restriction. When $f(\alpha) < 0$, the corresponding $\alpha$s, called *latent*, are rare coarse exponents, which appear in few draws of the random measure and control high and low moments (Mandelbrot, 1989b). Similarly, since canonical measures allow $M$ to be greater than 1, the low-frequency average $\alpha_{k,L}(t)$ can be negative with positive probability. $(D3)$ thus defines the multifractal spectrum for negative, or *virtual*, values of $\alpha$. This topic, further discussed in Mandelbrot (1989b), remains an active research area in mathematics.

[50] It is easy to show that $\alpha_0 q - \tau(q)$ is minimal for $q = 0$. The set $T(\alpha_0)$ has therefore fractal dimension $f(\alpha_0) = -\tau(0) = 1$, and thus carries all of the Lebesgue measure. Moreover by the Central Limit Theorem, $f(\alpha)$ is locally quadratic around $\alpha_0$, as shown in CFM.

## References


[1] Adelman, I. (1965), Long Cycles: Fact or Artefact?, *American Economic Review* **55**, 444-463

[2] Andersen, T. and T. Bollerslev (1997), Heterogeneous Information Arrivals and Return Volatility Dynamics: Uncovering the Long-Run in High Frequency Returns, *Journal of Finance* **52**, 975-1005

[3] Avery, C., and Zemsky, P. (1998), Multidimensional Uncertainty and Herd Behavior in Financial Markets, *American Economic Review* **88**, 724-748

[4] Backus, D. K., and Zin, S. E. (1993), Long Memory Inflation Uncertainty: Evidence from the Term Structure of Interest Rates, *Journal of Money, Credit and Banking* **25**, 681-700

[5] Baillie, R. T. (1996), Long Memory Processes and Fractional Integration in Econometrics, *Journal of Econometrics* **73**, 5-59

[6] Baillie, R. T., Bollerslev, T., and Mikkelsen, H. O. (1996), Fractionally Integrated Generalized Autoregressive Conditional Heteroskedasticity, *Journal of Econometrics* **74**, 3-30

[7] Baillie, R. T., Chung, C. F., and Tieslau, M. A. (1996), Analyzing Inflation by the Fractionally Integrated ARFIMA-GARCH Model, *Journal of Applied Econometrics* **11**, 23-40

[8] Bates, D. S. (1995), Testing Option Pricing Models, *NBER Working Paper No. 5129*

[9] Bates, D. S. (1996), Jumps and Stochastic Volatility: Exchange Rate Process Implicit in Deutsche Mark Options, *Review of Financial Studies* **9**, 69-107

[10] Belkacem, L., Lévy-Véhel, J., and Walter, C. (1995), Generalized Market Equilibrium: "Stable" CAPM, Working Paper presented at the AFFI-International Conference of Finance 1995 held in Bordeaux, France

[11] Beveridge, W. H. (1925), Weather and Harvest Cycles, *Economic Journal* **31**, 429-452

[12] Bikhchandani, S., Hirshleifer, D., and Welch, I. (1992), A Theory of Fads, Fashion, Custom and Cultural Change as Informational Cascades, *Journal of Political Economy* **100**, 992-1027

[13] Billingsley, P. (1979), *Probability and Measure*, New York: John Wiley and Sons

[14] Bochner, S. (1955), *Harmonic Analysis and the Theory of Probability*, Berkeley: University of California Press

[15] Bollerslev, T. (1986), Generalized Autoregressive Conditional Heteroskedasticity, *Journal of Econometrics* **31**, 307-327

[16] Bollerslev, T. (1987), A Conditional Heteroskedastic Time Series Model for Speculative Prices and Rates of Return, *Review of Economics and Statistics* **69**, 542-547

[17] Boudoukh, J., Richardson, M., and Whitelaw, R. (1994), A Tale of Three Schools: Insights on Autocorrelations of Short-Horizon Returns, *Review of Financial Studies* **7**, 539-573

[18] Breidt, J., Crato, N., and DeLima, P. (1998), On the Detection and Estimation of Long-Memory in Stochastic Volatility, forthcoming, *Journal of Econometrics*

[19] Bulow, J., and Klemperer, P. (1994), Rational Frenzies and Crashes, *Journal of Political Economy* **102**, 1-24

[20] Calvet, L. (1998), *Incomplete Markets and Volatility*, Ch. 1 in Ph. D. Dissertation, Yale University. Paper available from the SSRN database: http://www.ssrn.com

[21] Calvet, L., Fisher, A., and Mandelbrot, B. B. (1997), Large Deviation Theory and the Distribution of Price Changes, *Cowles Foundation Discussion Paper No. 1165*, Yale University, Paper available from the SSRN database: http://www.ssrn.com

[22] Campbell, J., Lo, A., and MacKinlay, A. C. (1997), *The Econometrics of Financial Markets*, Princeton University Press

[23] Clark, P. K. (1973), A Subordinated Stochastic Process Model with Finite Variance for Speculative Prices, *Econometrica* **41**, 135-156

[24] Cox, J. C., Ingersoll, J. E., and S. A. Ross (1985), An Intertemporal General Equilibrium Model of Asset Prices, *Econometrica* **53**, 363-84

[25] Dacorogna, M. M., Müller, U. A., Nagler, R. J., Olsen, R. B., and Pictet, O. V. (1993), A Geographical Model for the Daily and Weekly Seasonal Volatility in the Foreign Exchange Market, *Journal of International Money and Finance* **12**, 413-438

[26] Diebold, F. X., and Rudebusch, G. D. (1989), Long Memory and Persistence in Aggregate Output, *Journal of Monetary Economics* **24**, 189-209

[27] Ding, Z., Granger, C. W. J., and Engle, R. F. (1993), A Long Memory Property of Stock Returns and a New Model, *Journal of Empirical Finance* **1**, 83-106

[28] Dothan, M. (1990), *Prices in Financial Markets*, Oxford University Press

[29] Drost, F. C., and Nijman, T. E. (1993), Temporal Aggregation of GARCH Processes, *Econometrica* **61**, 909-927

[30] Durrett, R. (1991), *Probability: Theory and Examples*, Pacific Grove, Calif.: Wadsworth & Brooks/Cole Advanced Books & Software

[31] Engle, R. F. (1982), Autoregressive Conditional Heteroscedasticity with Estimates of the Variance of United Kingdom Inflation, *Econometrica* **50**, 987-1007

[32] Engle, R. F., and Gonzalez-Rivera, G. (1991), Semiparametric ARCH Models, *Journal of Business and Economic Statistics* **9**, 345-359

[33] Engle, R. F., and Lee, G. J. (1996), Estimating Diffusion Models of Stochastic Volatility, in *Modelling Stock Market Volatility: Bridging the Gap to Continuous Time* 333-356, New York: Academic Press

[34] Evertsz, C. J. G., and Mandelbrot, B. B. (1992), Multifractal Measures, in: Peitgen, H. O., Jürgens, H., and Saupe, D. (1992), *Chaos and Fractals: New Frontiers of Science*, 921-953, New York: Springer Verlag

[35] Fama, E. F. (1963), Mandelbrot and the Stable Paretian Hypothesis, *Journal of Business* **36**, 420-429

[36] Feller, W. (1971), *An Introduction to Probability Theory and its Applications*, New York: John Wiley and Sons

[37] Fisher, A., Calvet, L., and Mandelbrot, B. B. (1997), Multifractality of Deutschmark/US Dollar Exchange Rates, *Cowles Foundation Discussion Paper No. 1166*, Yale University. Paper available from the SSRN database: http://www.ssrn.com

[38] Frisch, U., and Parisi, G. (1985), Fully Developed Turbulence and Intermittency, in: M. Ghil ed., *Turbulence and Predictability in Geophysical Fluid Dynamics and Climate Dynamics*, 84-88, Amsterdam: North-Holland

[39] Gennotte, G., and Leland, H. (1990), Market Liquidity, Hedging and Crashes, *American Economic Review* **80**, 999-1021

[40] Ghysels, E., Gouriéroux, C., and Jasiak, J. (1995), Market Time and Asset Price Movements: Theory and Estimation, *CIRANO and CREST Discussion Paper*

[41] Ghysels, E., Gouriéroux, C., and Jasiak, J. (1996), Trading Patterns, Time Deformation and Stochastic Volatility in Foreign Exchange Markets, *CREST Working Paper n° 9655*

[42] Glosten, L. Jagannathan, R., and D. Runkle (1993), On the Relation Between the Expected Value and the Volatility of the Nominal Excess Return on Stocks, *Journal of Finance* **48**, 1779-1801

[43] Granger, C. W. J., and Joyeux, R. (1980), An Introduction to Long Memory Time Series Models and Fractional Differencing, *Journal of Time Series Analysis* **1**, 15-29

[44] Guivarc'h, Y. (1987), Remarques sur les Solutions d'une Equation Fonctionnelle Non Linéaire de Benoit Mandelbrot, *Comptes Rendus (Paris)* **3051**, 139

[45] Halsey, T. C., Jensen, M. H., Kadanoff, L. P., Procaccia, I., and Shraiman, B. I. (1986), Fractal Measures and their Singularities: The Characterization of Strange Sets, *Physical Review Letters A* **33**, 1141

[46] Harrison, J. M., and Kreps, D. (1979), Martingales and Arbitrage in Multiperiod Securities Markets, *Journal of Economic Theory* **20**, 381-408

[47] Hosking, J. R. M. (1981), Fractional Differencing, *Biometrika* **68**, 165-176

[48] Jacklin, C., Kleidon, A., and Pfleiderer, P. (1992), Underestimation of Portfolio Insurance and the Crash of October 1987, *Review of Financial Studies* **5**, 35-63

[49] Kahane, J. P. (1997), A Century of Interplay Between Taylor Series, Fourier Series and Brownian Motion, *Bulletin of the London Mathematical Society* **29**, 257-279

[50] Koedjik, K. G., and Kool, C. J. M. (1992), Tail Estimates of East European Exchange Rates, *Journal of Business and Economic Statistics* **10**, 83-96

[51] Mandelbrot, B. B. (1963), The Variation of Certain Speculative Prices, *Journal of Business* **36**, 394-419

[52] Mandelbrot, B. B. (1965), Une Classe de Processus Stochastiques Homothétiques a Soi, *Comptes Rendus de l'Académie des Sciences de Paris* **260**, 3274-3277

[53] Mandelbrot, B. B. (1969), Long-Run Linearity, Locally Gaussian Process, *H*-Spectra and Infinite Variances, *International Economic Review* **10**, 82-111

[54] Mandelbrot, B. B. (1971), Statistical Dependence in Prices and Interest Rates, *Fifty First Annual Report of the National Bureau of Economic Research*, 141-142

[55] Mandelbrot, B. B. (1972a), Statistical Methodology for Nonperiodic Cycles: From the Covariance to $R/S$ Analysis, *Annals of Economic and Social Measurement*, **1/3**, 259-290

[56] Mandelbrot, B. B. (1972b), Possible Refinements of the Lognormal Hypothesis Concerning the Distribution of Energy Dissipation in Intermitent Turbulence, in: M. Rosenblatt and C. Van Atta eds., *Statistical Models and Turbulence*, New York: Springer Verlag

[57] Mandelbrot, B. B. (1973), Comments on "A Subordinated Stochastic Process with Finite Variance for Speculative Prices" by Peter K. Clark, *Econometrica* **41**, 157-160

[58] Mandelbrot, B. B. (1974), Intermittent Turbulence in Self-Similar Cascades: Divergence of High Moments and Dimension of the Carrier, *Journal of Fluid Mechanics* **62**, 331-358

[59] Mandelbrot, B. B. (1982), *The Fractal Geometry of Nature*, New York: Freeman

[60] Mandelbrot, B. B. (1989a), Multifractal Measures, Especially for the Geophysicist, *Pure and Applied Geophysics* **131**, 5-42

[61] Mandelbrot, B. B. (1989b), Examples of Multinomial Multifractal Measures that Have Negative Latent Values for the Dimension $f(\alpha)$, in: L. Pietronero ed., *Fractals'Physical Origins and Properties,* 3-29, New York: Plenum

[62] Mandelbrot, B. B. (1997), *Fractals and Scaling in Finance: Discontinuity, Concentration, Risk*, New York: Springer Verlag

[63] Mandelbrot, B. B., Fisher, A., and Calvet, L. (1997), The Multifractal Model of Asset Returns, *Cowles Foundation Discussion Paper No. 1164*, Yale University. Paper available from the SSRN database: http://www.ssrn.com

[64] Mandelbrot, B. B., and Ness, J. W. van (1968), Fractional Brownian Motion, Fractional Noises and Application, *SIAM Review* **10**, 422-437

[65] Mandelbrot, B. B. and Taylor, H. W. (1967), On the Distribution of Stock Price Differences, *Operations Research* **15**, 1057-1062

[66] Mandelbrot, B. B., and Wallis, J. R. (1969), Some Long Run Properties of Geophysical Records, *Water Resources Research* **5**, 321-340

[67] Merton, R. C. (1990), *Continuous-Time Finance*, Cambridge, Mass. : Blackwell

[68] Müller, U. A., Dacorogna, M. M., Davé, R. D., Pictet, O. V., Olsen, R. B., and Ward, J. R. (1995), *Fractals and Intrinsic Time: A Challenge to Econometricians*, Discussion Paper Presented at the 1993 International Conference of the Applied Econometrics Association held in Luxembourg

[69] Nelson, D. B. (1991), Conditional Heteroskedasticity in Asset Returns: A New Approach, *Econometrica* **45**, 7-38

[70] Peyrière, J. (1991), Multifractal Measures, in *Proceedings of the NATO ASI "Probabilistic Stochastic Methods in Analysis, with Applications"*

[71] Phillips, P. C. B., McFarland, J. W., and McMahon, P. C. (1994), Robust Tests of Forward Exchange Market Efficiency with Empirical Evidence from the 1920's, *Journal of Applied Econometrics* **11**, 1-22

[72] Rossi, P. ed. (1997), *Modeling Stock Market Volatility: Bridging the Gap to Continuous Time*, New York: Academic Press

[73] Samorodnitsky, G., and Taqqu, M. S. (1994), *Stable Non-Gaussian Random Processes*, New York: Chapman and Hall

[74] Sowell, F. B. (1992), Modeling Long Run Behavior with the Fractional ARIMA Model, *Journal of Monetary Economics* **29**, 277-302

[75] Stock, J. H. (1987), Measuring Business Cycle Time, *Journal of Political Economy* **95**, 1240-1261

[76] Stock, J. H. (1988), Estimating Continuous-Time Processes Subject to Time Deformation, *Journal of the American Statistical Association* **83**, 77-85

[77] Taqqu, M. S. (1975), Weak Convergence to Fractional Brownian Motion and to the Rosenblatt Process, *Z. Wahrscheinlichkeitstheorie verw. Gebiete* **31**, 287-302

[78] Taylor, S. (1986), *Modelling Financial Time Series*, New York: Wiley

[79] Wiggins, J. B. (1987), Option Values under Stochastic Volatility: Theory and Empirical Estimates, *Journal of Financial Economics* **19**, 351-372.

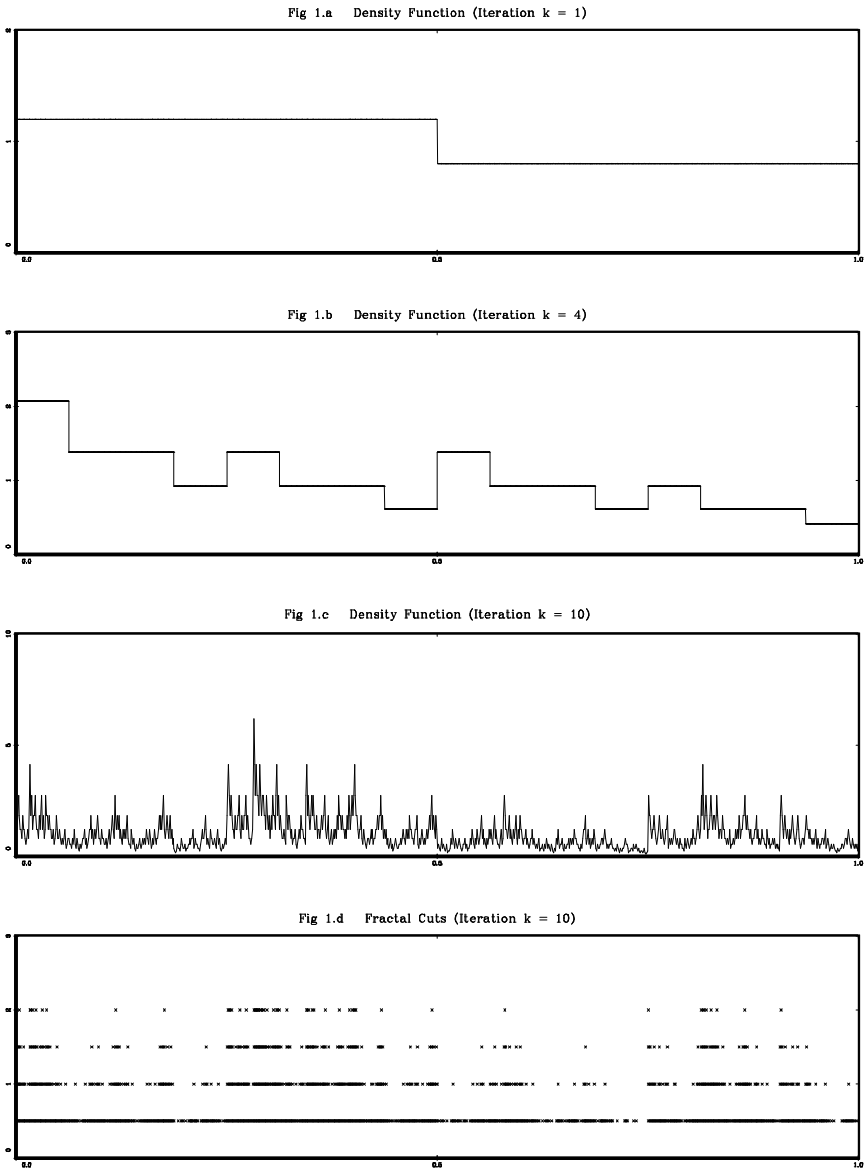


**Figure 1: Construction of the Binomial Measure.** In panels (a) and (b), the construction is deterministic with the fraction $m_0 = 0.6$ of the mass always allocated to the left, and fraction $m_1 = 0.4$ always allocated to the right. Panel (c) shows a randomized binomial measure after $k = 10$ stages. The masses $m_0$ and $m_1$ each have equal probabilities of going to the left or right. The final panel shows the fractal character of "cuts" of various sizes. Each cut shows the set of instants at which the random measure in panel (c) exceeds a given level. The clustering of these sets has a silf-similar structure, and the extreme bursts of volatility are intermittent, as discussed in Appendix 8.6.

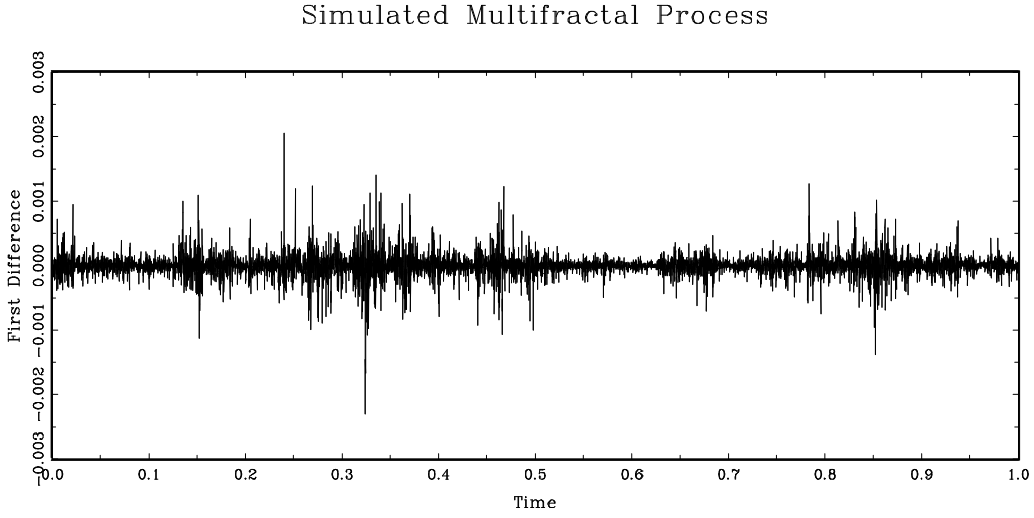


**Figure 2: MMAR Simulations with Random Binomial Trading Time.** This figure shows the first differences of simulations obtained by compounding a standard Brownian Motion with a binomial trading time. The simulations display volatility clustering at all time scales and intermittent large fluctuations.

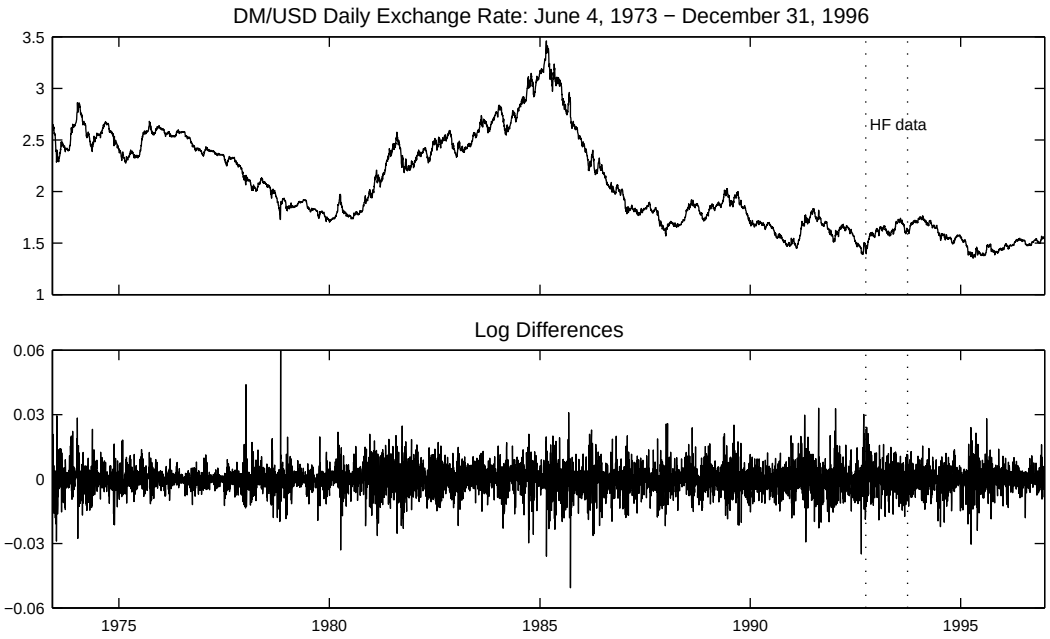


**Figure 3: DM/USD Daily Data.** The data is provided by Olsen and Associates and spans from June 1973 to December 1996. The outlined area labeled "HF data" shows the one year period from October 1992 to October 1993 that corresponds to the span of our high-frequency data. Despite the apparent long-cycles and clustering of volatility in the daily data, the MMAR provides sufficient flexibility to capture this behavior in a parsimonious stationary model. Moreover, both the daily data and the high-frequency data show similar scaling patterns.

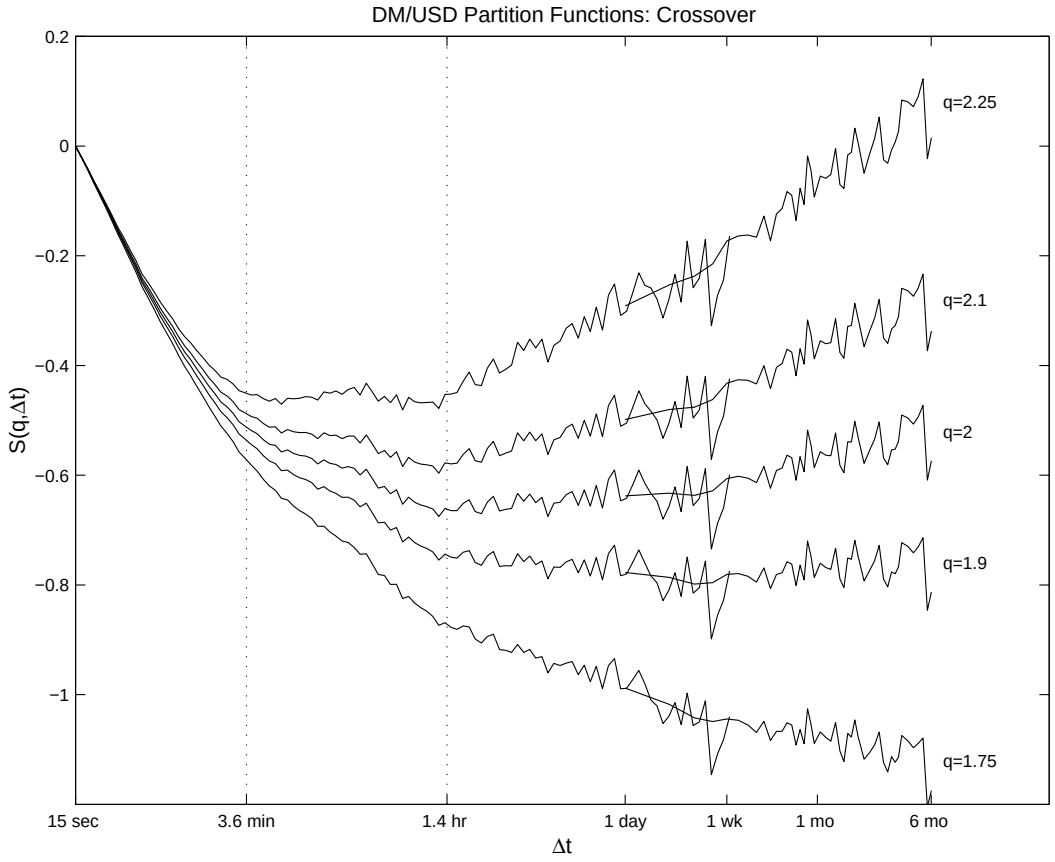


**Figure 4: DM/USD Partition Functions for the full set of time scales and moments $q$ near 2.** This figure shows high-frequency crossover in the DM/USD data. We identify a scaling region from about 1.4 hours to at least six months, the largest horizon for which the partition function was calculated. High-frequency crossover is caused by market frictions such as bid-ask spread, discreteness of trading units, and non-continuous trade. Choosing moments $q$ near 2 allows us to test the martingale hypothesis for returns since the slope $\tau(q = 1/H) = 0$. We find a flat slope near $q = 1.88$, implying $\widehat{H} = 0.53$, or slight persistence. We do not report standard errors, but this is close to the value $H = 1/2$ predicted by the martingale hypothesis.

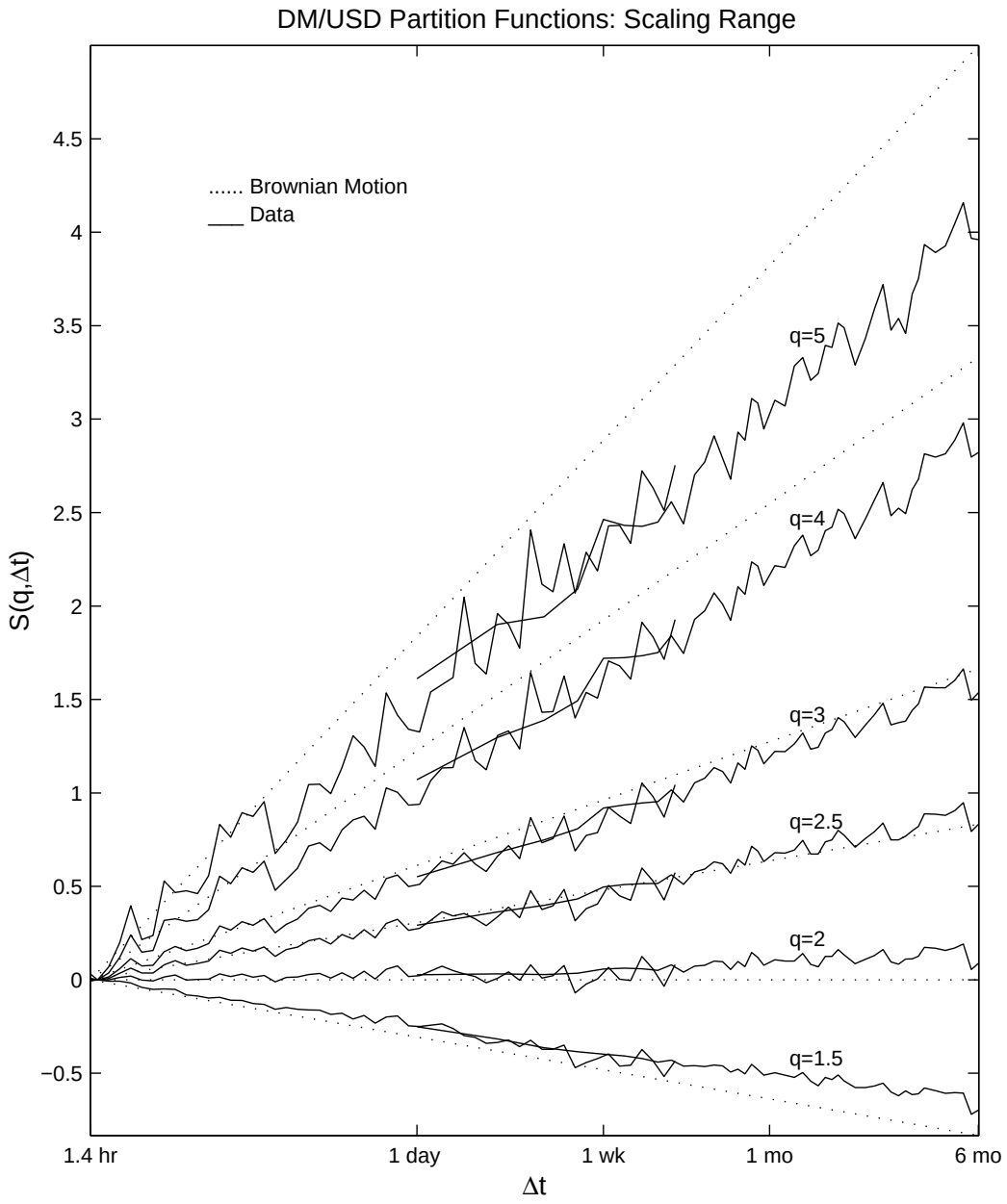


**Figure 5: DM/USD Partition Functions in the scaling region for moments** $1.5 \leq q \leq 5$**.** For each moment, the first solid line plotted from 1.4 hours to two weeks corresponds to the high-frequency data. The second solid line ranges from $\Delta t = 1$ day to 6 months, and corresponds to the daily data. The lines are remarkably straight, as predicted by the model, and have nearly identical slopes. Also, their scaling is noticeably different from that of the Brownian Motion, which is shown by the dotted lines in the figure.

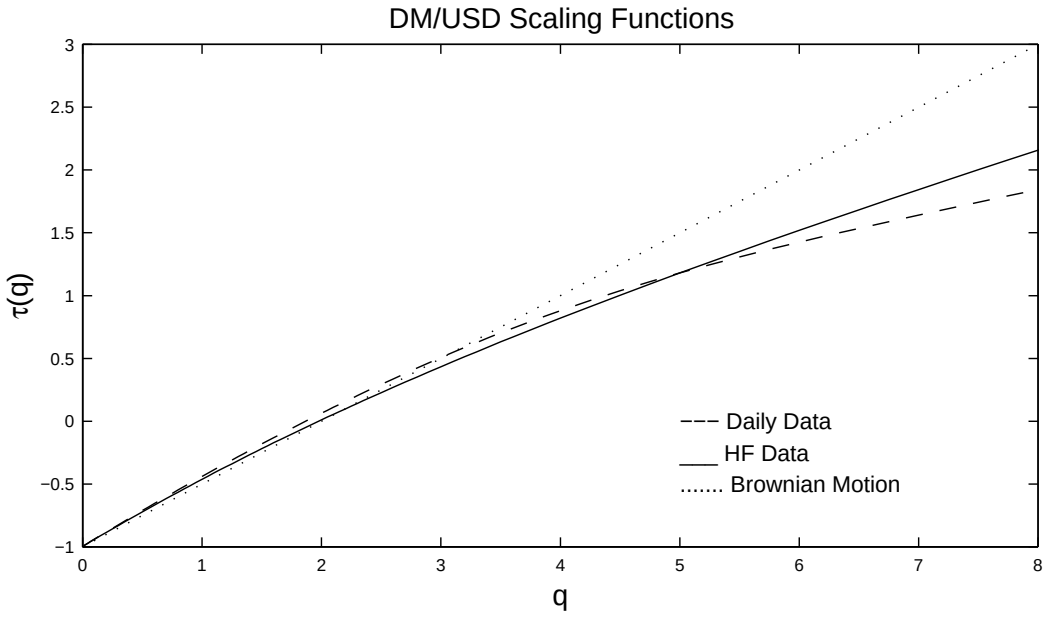


**Figure 6: Estimated DM/USD Scaling Functions.** For each partition function $S_q(T, \Delta t)$ we estimate the slope using OLS to obtain $\widehat{\tau}_X(q)$. The estimated scaling functions for both data sets are concave, and have a similar shape until high moments are reached. The contrast with Brownian Motion is shown by the dotted line.

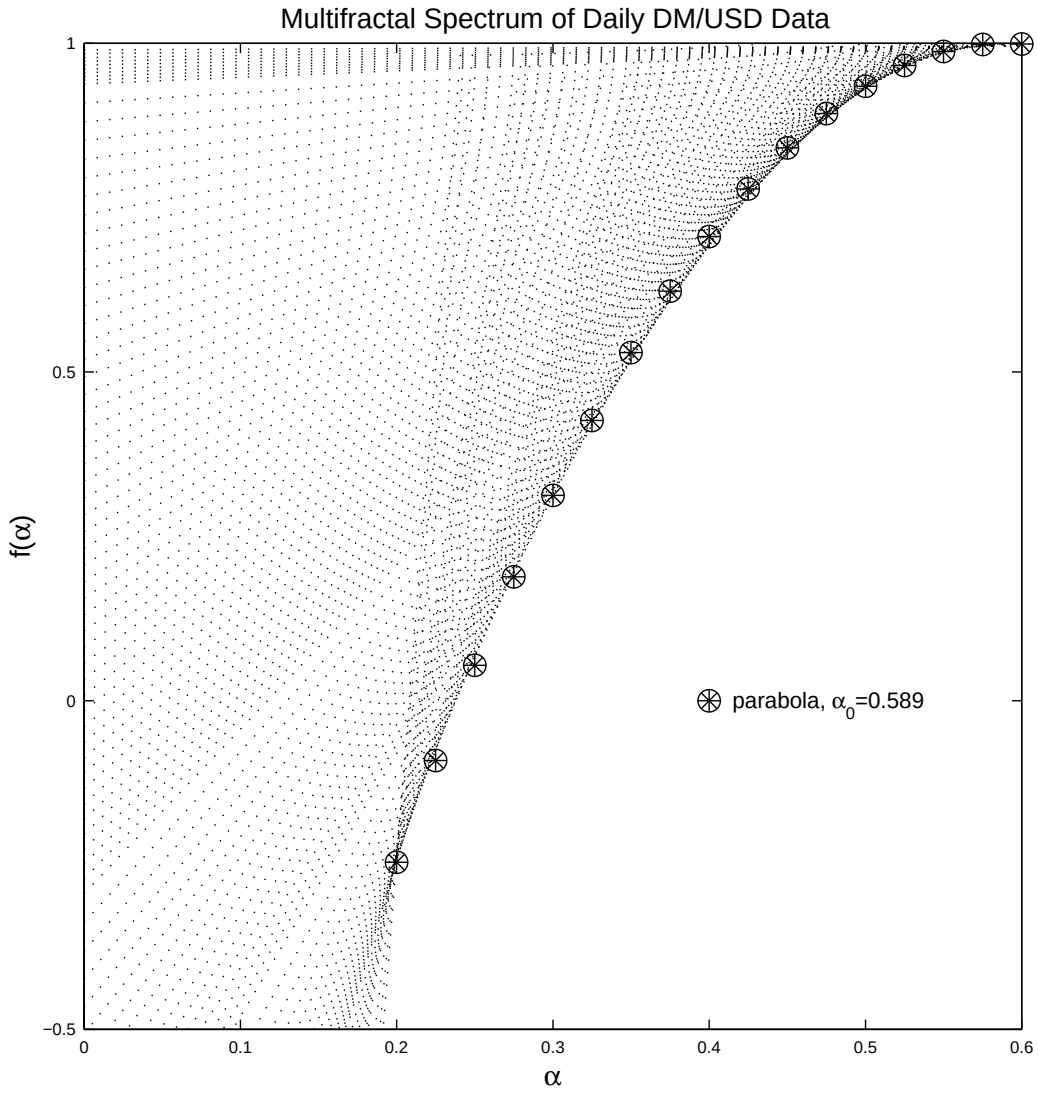


**Figure 7: Estimated Multifractal Spectrum of Daily DM/USD Data.** The estimated spectrum is obtained from the Legendre transform $\widehat{f}_X(\alpha) = \inf_q [\alpha q - \widehat{\tau}(q)]$, shown in this graph by the lower envelope of the dotted lines. The shape is nearly quadratic, with the best fit shown by the marked symbols. A quadratic spectrum implies a lognormal distribution for multipliers $M$ in the multifractal generating mechanism.

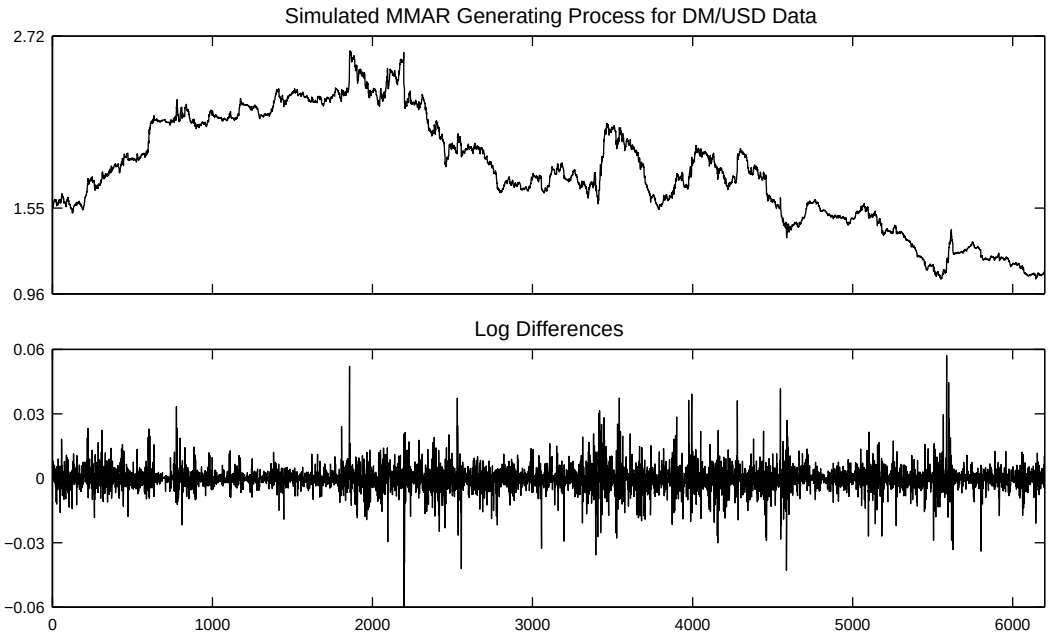


**Figure 8: Simulated Multifractal Generating Process for the DM/USD Data.** We use the estimated values of $\widehat{H} = 0.53$ and $\widehat{\alpha}_0 = 0.589$ with the limit lognormal construction of trading time. The plots show volatility clustering at all time scales and occasional large fluctuations.

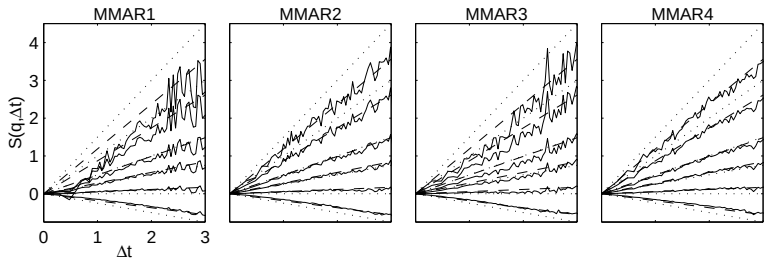


(a) MMAR Simulations

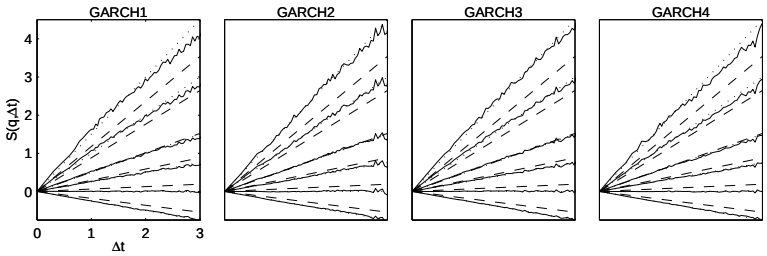


(b) GARCH Simulations

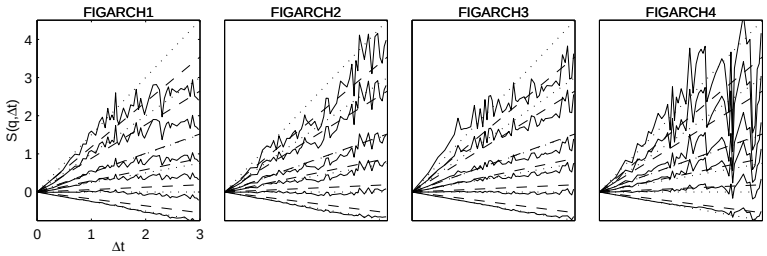


(c) FIGARCH Simulations

**Figure 9: Simulated Partition Functions.** Each panel shows estimated partition functions for a simulated sample of 100,000 observations. The multifractal data generating process in (a) uses our estimates. The data generating processes in (b) and (c) use specifications from previously published research on daily DM/USD exchange rates. Large simulated samples are used to reduce variability as much as possible and obtain the expected scaling properties of each process. Dotted lines in each figure represent the scaling predicted for Brownian Motion, and dashed lines represent the scaling found in the data. The MMAR appears most likely to capture scaling in the DM/USD data, as expected from its construction. Nonetheless, at smaller sample sizes comparable to the daily DM/USD data, MMAR simulations tend to be more variable than both the data and the examples above. This suggests either bias in our estimation method, or possibly that the data generating process has stronger scaling features than our model. The GARCH simulations tend to scale like Brownian Motion, but with some slight bend in the partition functions. FIGARCH simulations occasionally show scaling that is similar to the data, as in panel c2, but in general tend to be much more irregular.

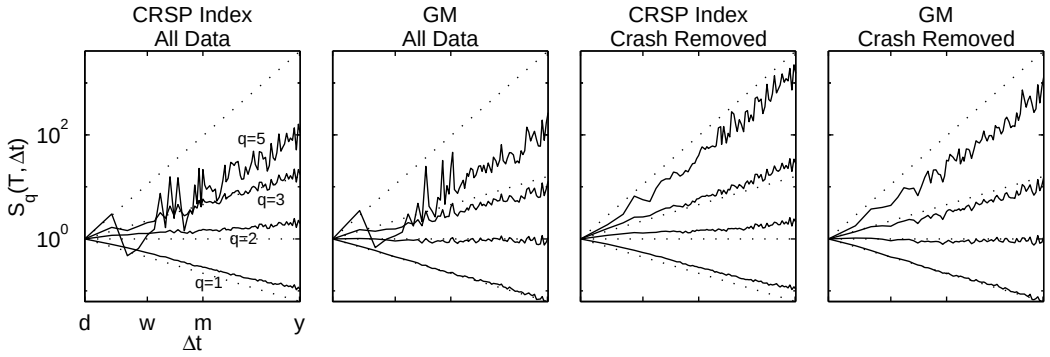


**Figure 10: Partition Functions for CRSP Index and GM.** The data spans from 1962 to 1998, and the time increments labeled "d", "w", "m", and "y" correspond to one day, one week, one month, and one year respectively. When the full data sets are used, we observe scaling in the first three moments, and for horizons $\Delta t \geq 3$ days in the fifth moments. The drop in the fifth moments between two and three days is caused by sharp rebounds for both series from the 1987 crash. After removing the crash from the data, the second two panels show striking linearity, but change the slopes of the full-sample plots to increase and thus appear more Brownian.

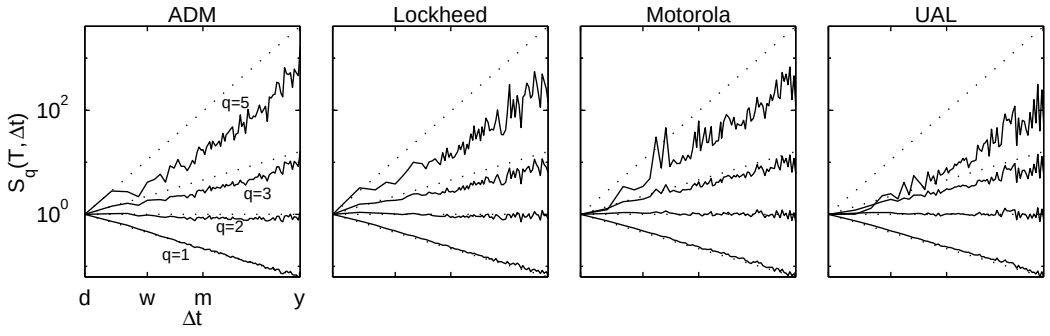


**Figure 11: Partition Functions for ADM, Lockheed, Motorola, and UAL.** Each of these show strong scaling properties despite the 1987 crash.